

**Cobalt-Catalyzed  $[2\pi+2\pi]$  Cycloadditions of Alkenes: Scope,  
Mechanism and Elucidation of Electronic Structure of Catalytic  
Intermediates.**

*Valerie A. Schmidt, Jordan M. Hoyt, Grant W. Margulieux, and Paul J. Chirik*

*Department of Chemistry*

*Princeton University, Princeton, NJ 08544, United States*

*Supporting Information*

## Table of Contents

I. Experimental Section	S3
A. General Considerations	S3
B. Preparation of Ligands	S5
C. Preparation of Cobalt Compounds	S7
D. Preparation of Substrates	S10
E. Preparation and Characterization of Cyclobutane Products	S11
II. Additional X-ray Crystallographic Data	S14
III. Electrochemical Data	S23
IV. EPR Spectroscopic Data	S24
V. Additional Kinetic Data	S31
VI. Additional Computational Results	S35
VII. References	S41
VIII. $^1\text{H}$ and $^{13}\text{C}$ NMR Spectra of Organic Compounds	S43

## I. Experimental Section

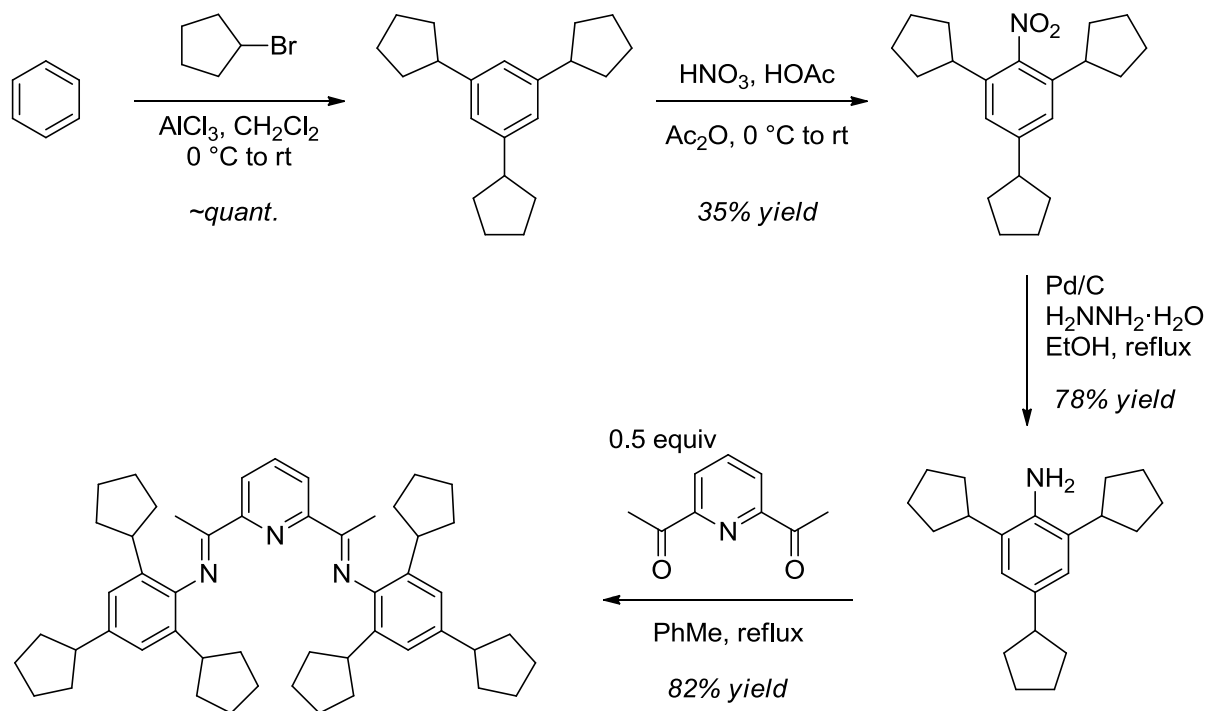
**A. General Considerations.** All air- and moisture-sensitive manipulations were carried out using standard high vacuum line, Schlenk or cannula techniques or in an M. Braun inert atmosphere drybox containing an atmosphere of purified nitrogen. The M. Braun drybox was equipped with a cold well designed for freezing samples in liquid nitrogen. Solvents for air- and moisture-sensitive manipulations were dried and deoxygenated using literature procedures.<sup>1</sup> Deuterated solvents for NMR spectroscopy were distilled from sodium metal under an atmosphere of argon and stored over 4 Å molecular sieves. The ligands (<sup>i</sup>PrPDI), <sup>Me</sup>PDI, <sup>i</sup>PrEtPDI, 4-pyrr(<sup>i</sup>PrPDI) were prepared according to literature procedures.

<sup>1</sup>H and <sup>13</sup>C NMR were recorded at 400 and 126 MHz, respectively. All chemical shifts are reported relative to SiMe<sub>4</sub> using <sup>1</sup>H (residual) chemical shifts of the solvent as a secondary standard. Infrared spectroscopy was conducted on a Thermo-Nicolet iS10 FT-IR spectrometer calibrated with a polystyrene standard. Elemental analyses were performed at Robertson Microlit Laboratories, Inc., in Ledgewood, NJ. GC analyses were performed using a Shimadzu GC-2010 gas chromatograph equipped with a Shimadzu AOC-20s autosampler and Shimadzu SHRXI-5MS capillary column (15 m x 250µm). Continuous wave EPR spectra were recorded at room temperature, unless otherwise noted, on an X-band Bruker EMXPlus spectrometer equipped with an EMX standard resonator and a Bruker PremiumX microwave bridge. The spectra were simulated using EasySpin for MATLAB.<sup>2</sup> Solid state magnetic moments were determined using a Johnson Matthey Magnetic Susceptibility Balance, collected at room temperature, unless otherwise noted. High-resolution mass spectra were measured using a Agilent 6210 Accurate-Mass TOF LC-MS. The mass spectrometer was calibrated externally before each use with purine and the Agilent ES-TOF tuning mix (part number = G1969-85000). These compounds were assigned a (M+H)<sup>+</sup> *m/z* ratio of 121.050873 and 922.009798 respectively.

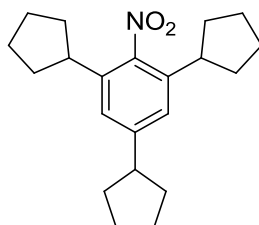
Single crystals suitable for X-ray diffraction were coated with polyisobutylene oil in a drybox, transferred to a nylon loop and then quickly transferred to the goniometer head of a Bruker X8 APEX2 diffractometer equipped with molybdenum and copper X-ray tubes ( $\lambda$  = 0.71073 and 1.54184 Å, respectively). Preliminary data revealed the crystal system. The data collection strategy was optimized for completeness and redundancy using the Bruker COSMO software suite. The space group was identified, and the data were processed using the Bruker SAINT+ program and corrected for absorption using SADABS. The structures were solved using direct methods (SHELXS) completed by subsequent Fourier synthesis and refined by full-matrix least-squares procedures.

All DFT calculations were performed with the ORCA program package in the gas phase.<sup>3</sup> The geometry optimizations of the complexes and single point calculations on the optimized geometries were carried out on the B3LYP level of DFT.<sup>4,5,6</sup> This hybrid functional often gives better results for transition metal compounds than pure gradient-corrected functionals, especially with regard to metal-ligand covalency.<sup>7</sup> The all-electron Gaussian basis sets were those developed by Ahlrichs' group.<sup>8,9,10</sup> Triple- $\xi$  quality basis sets def2-TZVP with one set of polarization functions on the metals and on the atoms directly coordinated to the metal center were used. For the carbon and hydrogen atoms, slightly smaller polarized split-valence def2-SV(P) basis sets were used that were of double- $\xi$  quality in the valence region and contained a polarizing set of d functions on the non-hydrogen atoms. Auxiliary basis sets were chosen to match the orbital basis.<sup>11,12,13</sup> The RIJCOSX<sup>14,15,16</sup> approximation was used to accelerate the calculations. Throughout this manuscript, computational results are described using the broken symmetry approach by Ginsberg<sup>17</sup> and Noodleman et al.<sup>18</sup> Because several broken symmetry solutions to the spin-unrestricted Kohn-Sham equations may be obtained, the general notation broken symmetry  $(m,n)$ <sup>19</sup> has been adopted, where  $m$  ( $n$ ) denotes the number of spin-up (spin-down) electrons at the two interacting fragments.<sup>20</sup> Canonical and corresponding orbitals, as well as spin density plots, were generated with the program *Chimera*.<sup>21</sup>

**B. Preparation of Ligands.** The ligands <sup>iPr</sup>PDI, <sup>Me</sup>PDI, <sup>Et</sup>PDI, <sup>iPr</sup>EtPDI, <sup>iPr</sup><sub>2</sub>iPrPDI,<sup>22</sup> 4-pyrr(<sup>iPr</sup>PDI)<sup>23</sup> were prepared according to literature procedures. (<sup>Tric</sup>PDI) was synthesized as shown below:

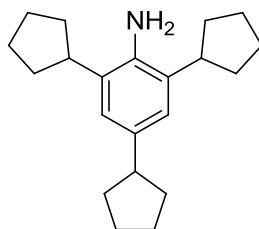


1,3,5-tricyclopentylbenzene was synthesized via Friedel-Crafts alkylation of benzene with bromocyclopentane and AlCl<sub>3</sub> using the procedure outlined by Buchwald and co-workers.<sup>24</sup>



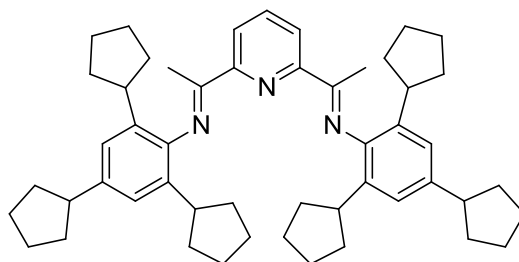
**Preparation of 1,3,5-tricyclopentyl-2-nitrobenzene.** To a solution of 1,3,5-tricyclopentylbenzene (6.62 g, 23.4 mmol, 1.0 equiv) and acetic anhydride (2.60 mL) 0 °C was added a mixture of fuming nitric acid (1.56 mL, 36.6 mmol, 1.56 equiv), acetic anhydride (886 μL, 9.37 mmol, 0.40 equiv), and acetic acid (989 μL, 15.7 mmol, 0.67 equiv). The mixture was warmed to room temperature and stirred overnight before diluting with CH<sub>2</sub>Cl<sub>2</sub>, washing with a saturated NaHCO<sub>3</sub> solution (3x), brine, and drying the organic layer with Na<sub>2</sub>SO<sub>4</sub>. The concentrated organic material was purified via flash chromatography (5% EtOAc in hexanes) to isolate **1,3,5-tricyclopentyl-2-nitrobenzene** (2.68 g, 8.18 mmol, 35% yield) as a white solid.

Analytical data for **1,3,5-tricyclopentyl-2-nitrobenzene**:  $^1\text{H NMR}$  (500 MHz, chloroform-*d*)  $\delta$  ppm 1.54 - 1.77 (m, 12 H) 1.78 - 1.88 (m, 6 H) 2.01 - 2.13 (m, 6 H) 2.86 (quin,  $J=8.43$  Hz, 2 H) 3.00 (quin,  $J=9.60$  Hz, 1 H) 7.06 (s, 2 H);  $^{13}\text{C NMR}$  (126 MHz, chloroform-*d*)  $\delta$  25.45 (CH<sub>2</sub> on *para*-cyclopentyl), 25.60 (CH<sub>2</sub> on *ortho*-cyclopentyl), 34.66 (CH<sub>2</sub> on *para*-cyclopentyl), 34.89 (CH<sub>2</sub> on *ortho*-cyclopentyl), 40.50 (CH of *ortho*-cyclopentyl), 46.07 (CH of *para*-cyclopentyl), 123.07 (ArC-H), 136.91 (ArC-*para*-cyclopentyl), 148.57 (ArC-*ortho*-cyclopentyl), 149.91 (ArC-NO<sub>2</sub>); **HRMS** (ESI) Calc. for [C<sub>21</sub>H<sub>29</sub>NO<sub>2</sub>]<sup>+</sup> = 327.2198, Found = 327.2339.



**Preparation of 2,4,6-tricyclopentylaniline.** To a mixture of 1,3,5-tricyclopentyl-2-nitrobenzene (2.68 g, 8.18 mmol, 1 equiv) and 10% palladium on activated carbon (1.0 g) in EtOH (35 mL) was added hydrazine hydrate (30 mL), a reflux condenser attached, the system flushed with argon and heated to reflux for 16 hours. Complete conversion was determined by visualization using TLC, the reaction mixture cooled to room temperature and diluted with Et<sub>2</sub>O. The mixture was then washed with 1 M NaOH (2x), brine, then dried over Na<sub>2</sub>SO<sub>4</sub> and concentrated. The crude material was purified via flash chromatography (10% EtOAc in hexanes) to isolate **2,4,6-tricyclopentylaniline** (1.85 g, 6.22 mmol, 76% yield) as a viscous pale yellow oil.

Analytical data for **2,4,6-tricyclopentylaniline** :  $^1\text{H NMR}$  (500 MHz, chloroform-*d*)  $\delta$  ppm 1.54 - 1.63 (m, 3 H) 1.64 - 1.78 (m, 12 H) 1.78 - 1.90 (m, 5 H) 2.02 - 2.13 (m, 4 H) 2.92 (tt,  $J=9.93$ , 7.41 Hz, 1 H) 3.03 (quin,  $J=7.88$  Hz, 2 H) 3.69 (br. s., 2 H) 6.96 (s, 2 H);  $^{13}\text{C NMR}$  (126 MHz, chloroform-*d*)  $\delta$  25.24 (CH<sub>2</sub>), 25.45 (CH<sub>2</sub>), 32.40 (CH<sub>2</sub>), 34.92 (CH<sub>2</sub>), 40.43 (CH), 45.95 (CH), 122.11 (ArCH), 130.00 (ArC-cyclopentyl), 135.71 (ArC-cyclopentyl), 139.81 (ArC-NH<sub>2</sub>); **HRMS** (ESI) Calc. for [C<sub>21</sub>H<sub>31</sub>N]<sup>+</sup> = 297.2457, Found = 297.2454.

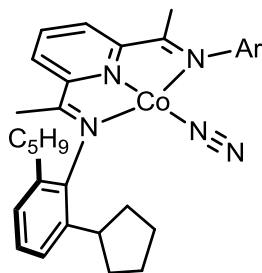


**Preparation of <sup>Tric</sup>PDI.** A mixture of 2,6-diacetylpyridine (495 mg, 3.03 mmol, 1.0 equiv), 2,4,6-tricyclopentylaniline (1.85 g, 6.22 mmol, 2.05 equiv), and a catalytic amount of p-toluene sulfonic acid (~10 mg) in PhMe (30 mL) were combined in a round-bottom flask, fitted with a Dean-Stark trap and reflux condenser and heated to reflux for 48 hours. The reaction mixture was cooled to room temperature, concentrated under reduced pressure, and the crude material recrystallized from MeOH to give <sup>tric</sup>PDI (1.79 g, 2.48 mmol, 82% yield) as a yellow crystalline solid.

Analytical data for <sup>Tric</sup>PDI: <sup>1</sup>H NMR (500 MHz, benzene-*d*<sub>6</sub>) δ ppm 1.34 - 1.45 (m, 8 H, cyclopentyl CH<sub>2</sub>) 1.56 - 1.80 (m, 28 H, cyclopentyl CH<sub>2</sub>) 1.85 - 1.94 (m, 4 H, cyclopentyl CH<sub>2</sub>) 2.03 - 2.14 (m, 8 H, cyclopentyl CH<sub>2</sub>) 2.37 (s, 6 H, imine CH<sub>3</sub>) 2.98 (quin, *J*=8.60 Hz, 2 H, *para*-cyclopentyl CH) 3.06 (quin, *J*=8.20 Hz, 4 H, *ortho*-cyclopentyl CH) 7.24 - 7.30 (overlapping s and t, 5 H, 4-pyridine-H and Ar-H) 8.58 (d, *J*=7.88 Hz, 2 H, 3,5-pyridine-H); <sup>13</sup>C NMR (126 MHz, benzene-*d*<sub>6</sub>) δ ppm 16.97 (cyclopentyl CH), 25.48, 25.65, 25.69, 33.78, 34.16, 35.06, 40.75 (cyclopentyl CH), 46.37 (imine CH<sub>3</sub>), 122.22 (aryl CH), 122.37 (aryl CH), 127.97 (pyridine CH), 133.35, 136.81 (pyridine CH), 141.08, 146.46, 155.47, 166.94 (imine carbonyl); Under ionization conditions this bis(imino)pyridine undergoes hydrolysis of one of the imine groups to give the pyridine imine-ketone and 2,4,6-tricyclopentylaniline which can be clearly detected by Hi-Res mass spectrometry. **HRMS** (ESI) Calc. for [C<sub>21</sub>H<sub>31</sub>N]<sup>+</sup> (aniline portion) = 297.2457, Found = 297.2454; Calc. for [C<sub>21</sub>H<sub>31</sub>N]<sup>+</sup> (pyridine imine-ketone portion) = 442.2984, Found = 442.2978.

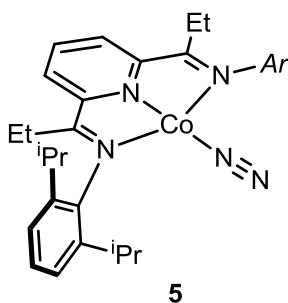
**C. Preparation of Cobalt Compounds.** The general procedure for the synthesis of (<sup>R</sup>PDI)CoN<sub>2</sub> compounds was followed as previously reported.<sup>2</sup>

Compound (<sup>Tric</sup>PDI)CoCl was observed during the reduction of (<sup>Tric</sup>PDI)CoCl<sub>2</sub> en route to **2**. (<sup>Tric</sup>PDI)CoCl: <sup>1</sup>H NMR (400 MHz, benzene-*d*<sub>6</sub>) δ ppm 0.18 (s, 6 H, imine CH<sub>3</sub>), 1.22 (m, *J*=6.61 Hz, 4 H, cyclopentyl-CH<sub>2</sub>), 1.34 (m, 4 H, cyclopentyl-CH<sub>2</sub>), 1.54 - 1.85 (m, 28 H, cyclopentyl-CH<sub>2</sub>), 1.86 - 2.15 (m, 12 H, cyclopentyl-CH<sub>2</sub>), 3.02 (m, *J*=7.03 Hz, 2 H, 4-cyclopentyl-CH), 3.46 - 3.59 (m, 4 H, 2,6-cyclopentyl-CH), 6.88 (d, *J*=7.67 Hz, 2 H, pyridine 3-CH), 7.39 (s, 4 H, aryl-CH), 9.42 (t, *J*=7.67 Hz, 1 H, pyridine 4-CH)



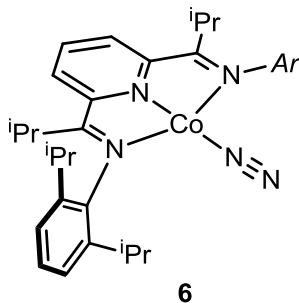
Compound (<sup>C<sup>5</sup>H<sup>9</sup></sup>PDI)CoN<sub>2</sub> was obtained using the reduction procedure outlined for **2** (see main text).

Analytical data for (<sup>C<sup>5</sup>H<sup>9</sup></sup>PDI)CoN<sub>2</sub> : Anal. Calcd for C<sub>41</sub>H<sub>51</sub>N<sub>5</sub>Co: C, 73.19; H, 7.64; N, 10.41. Found: C, 72.95; H, 7.74; N, 10.39. IR (pentane):  $\nu_{\text{NN}} = 2106 \text{ cm}^{-1}$ .



Compound **5** was obtained using the reduction procedure outlined for **2** (see main text).

Analytical data for (<sup>iPr</sup>EtPDI)CoN<sub>2</sub> (**5**): Anal. Calcd for C<sub>35</sub>H<sub>47</sub>N<sub>5</sub>Co: C, 70.45; H, 7.94; N, 11.74. Found: C, 70.68; H, 7.69; N, 10.99. IR (pentane):  $\nu_{\text{NN}} = 2100 \text{ cm}^{-1}$ .

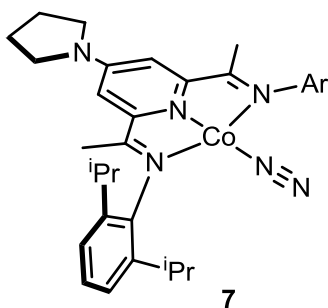


Compound **6** was obtained using the reduction procedure outlined for **2**, (see main text).

Analytical data for (<sup>iPr</sup>iPrPDI)CoN<sub>2</sub> (**6**): Anal. Calcd for C<sub>37</sub>H<sub>51</sub>N<sub>5</sub>Co: C, 71.13; H, 8.23; N, 11.21. Found: C, 70.98; H, 7.87; N, 10.83. IR (pentane):  $\nu_{\text{NN}} = 2100 \text{ cm}^{-1}$ .

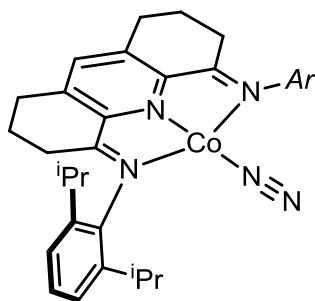


Analytical data for (<sup>iPr</sup>PDI)CoN<sub>2</sub> (**6**): Anal. Calcd for C<sub>37</sub>H<sub>51</sub>N<sub>5</sub>Co: C, 71.13; H, 8.23; N, 11.21. Found: C, 70.98; H, 7.87; N, 10.83. IR (pentane): ν<sub>NN</sub> = 2100 cm<sup>-1</sup>.



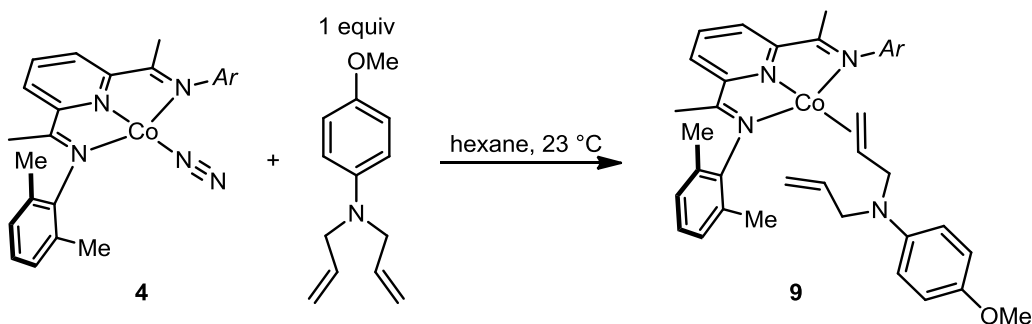
Compound **7** was obtained using the reduction procedure outlined for **2**, (see main text).

Analytical data for **4-pyrr**(<sup>iPr</sup>PDI)CoN<sub>2</sub> (**7**): Anal. Calcd for C<sub>37</sub>H<sub>50</sub>N<sub>6</sub>Co: C, 69.68; H, 7.90; N, 13.18. Found: C, 69.51; H, 7.86; N, 12.58. IR (pentane): ν<sub>NN</sub> = 2091 cm<sup>-1</sup>.



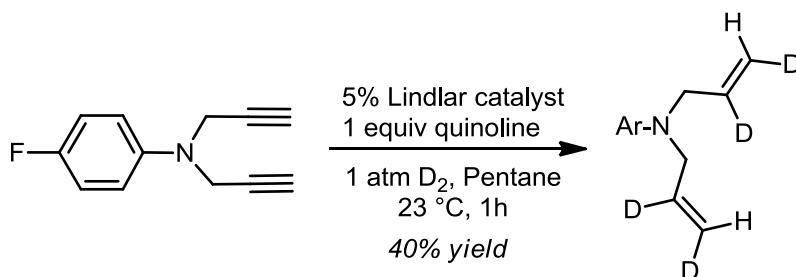
Compound (<sup>iPr</sup>tbPDI)CoN<sub>2</sub> was obtained using the reduction procedure outlined for **2**, (see main text).

Analytical data for (<sup>iPr</sup>tbPDI)CoN<sub>2</sub>: Anal. Calcd for C<sub>37</sub>H<sub>48</sub>N<sub>5</sub>Co: C, 71.48; H, 7.78; N, 11.26. Found: C, 71.23; H, 8.09; N, 10.83. IR (pentane): ν<sub>NN</sub> = 2088 cm<sup>-1</sup>



**Preparation of 9.** *N,N*-Diallyl-4-methoxyaniline (45 mg, 0.22 mmol, 1 equiv) was added via pipette to a suspension of **4** (100 mg, 0.22 mmol, 1 equiv) in hexane (approximately 1.5 mL). An immediate color change from teal to bright green was observed and pentane (2 mL) was added. The slurry was mixed for 5 minutes and the solid was collected by filtration. The solid was washed with pentane (1 mL) yielding **9** (0.083 g, 0.131 mmol, 60% yield) as a dark green solid. Anal. Calcd for C<sub>38</sub>H<sub>44</sub>N<sub>4</sub>OC<sub>o</sub>: C, 72.25; H, 7.02; N, 8.87. Found: C, 72.36; H, 6.88; N, 8.92. Magnetic Susceptibility Balance:  $\mu_{\text{eff}} = 2.5 \mu_{\text{B}}$  (23 °C). Toluene solution X-band EPR spectra of **9** was recorded at 295 K (microwave frequency = 9.37 GHz, power = 2.0 mW, modulation amplitude = 0.63 mT/100 kHz)  $g_{\text{iso}} = 2.04$ .

**D. Preparation of Substrates.** *N,N*-diallyl tritylamine,<sup>25</sup> *N,N*-diallyl-4-fluoroaniline,<sup>26</sup> *N,N*-diallyl-tert-butylamine,<sup>27</sup> *N,N*-diallyl benzylamine,<sup>27</sup> ethyl diallyl malonate (find this), diallyl fluorene,<sup>28</sup> (1-(allyloxy)allyl)benzene,<sup>29</sup> (1-(allyloxy)pro-2-ene-1,1-diyl)dibenzene<sup>30</sup> were synthesized via literature procedures. Allyl ether (Sigma-Aldrich) and 1,6-heptadiene (TCI America) were purchased from commercial sources. *N,N*-diallyl tritylamine was dried under high vacuum for 24 hours prior to use. All other substrates were dried over CaH<sub>2</sub> with stirring overnight followed by air-free vacuum distillation and were stored in a N<sub>2</sub> filled drybox prior to use.



*N,N*-dipropargyl-4-fluoroaniline was synthesized via propargylation of 4-fluoroaniline. Lindlar catalyst (283 mg) was added to a mixture of *N,N*-dipropargyl-4-fluoroaniline (500 mg, 2.67 mmol), quinolone (316  $\mu$ L, 2.67 mmol, 1.0 equiv), and pentane (40 mL) in a thick-walled glass pressure vessel and sealed. The mixture was frozen in liquid N<sub>2</sub> and evacuated, then filled with 1 atm of D<sub>2</sub>. The mixture was thawed and stirred at room temperature until the starting material was just consumed, about 1 hour, as judged by TLC. The mixture was then filtered through a plug of silica, concentrated, and the crude mixture was purified via flash chromatography (2.5% EtOAc/hexanes) to isolate *d*<sub>4</sub>-*N,N*-diallyl-4-fluoroaniline (208 mg, 1.06 mmol, 40% yield) as a clear, colorless oil.

**E. Preparation and Characterization of Cyclobutane Products.** *General [2+2] reaction conditions* : In a nitrogen-filled glovebox, a 20 mL scintillation vial was charged with (<sup>i</sup>PrPDI)CoN<sub>2</sub> (**1**) (5 mg, 0.00879 mmol, 0.025 equiv) and PhMe (0.2M, 1.7 mL) before α,ω-diene (0.352 mmol, 1 equiv) was added via microsyringe. The mixture was stirred at room temperature in the glovebox until substrate was completely consumed as judged by GC. The reaction mixture was then quenched by exposure to air, addition of 500 μL MeOH, and allowing the crude mixture to sit for 1 hour. Filtration through a short silica plug, flushing with additional MeOH, and concentrating under reduced pressure afforded analytically pure cyclobutane product.

The physical and analytical data for the azabicyclo[3.2.0]heptane products of *N,N*-diallyl *tert*-butylamine,<sup>27</sup> *N,N*-diallyl benzylamine,<sup>27</sup> allyl ether,<sup>31</sup> ethyl diallyl malonate,<sup>27</sup> diallylfluorene,<sup>32</sup> and 1,6-heptadiene<sup>27</sup> were identical to literature reported values.

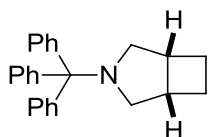


**Table 1, entry 1:** <sup>1</sup>H NMR (500 MHz, chloroform-*d*) δ ppm 1.53 (dd, *J*=9.14, 4.41 Hz, 2 H) 2.14 - 2.22 (m, 2 H) 2.24 - 2.32 (m, 2 H) 2.60 (m, 2 H) 3.02 (d, *J*=9.46 Hz, 2 H) 7.16 - 7.22 (m, 3 H) 7.27 - 7.33 (m, 6 H) 7.65 (d, *J*=7.57 Hz, 6 H). <sup>13</sup>C NMR (126 MHz, chloroform-*d*) δ 142.93 (Ar-C), 129.68 (Ar-CH), 127.21 (Ar-CH), 125.89 (Ar-CH), 73.88 (Trityl-C-N), 52.43 (N-CH<sub>2</sub>), 35.77 (cyclobutane CH), 23.95 (cyclobutane CH<sub>2</sub>); Under ionization conditions this compound fragments into two pieces which can be clearly detected by Hi-Res mass spectrometry. **HRMS** (ESI) Calc. for [C<sub>19</sub>H<sub>15</sub>]<sup>+</sup> = 243.1174, Found = 243.1176 (trityl portion), and Calc. for [C<sub>6</sub>H<sub>10</sub>N]<sup>+</sup> = 96.0813, Found = 96.0921 (bicycle-amine portion).

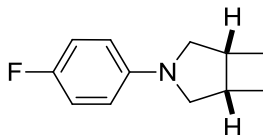


**Table 1, entry 3:** <sup>1</sup>H NMR (500 MHz, chloroform-*d*) δ ppm 1.83 (dt, *J* = 9.8, 5.0 Hz, 2H), 2.29 (dt, *J* = 9.9, 5.9 Hz, 2H), 3.00 (dd, *J* = 9.5, 4.8 Hz, 2H), 3.06 (dt, *J* = 6.8, 3.6 Hz, 2H), 3.48 (d, *J* = 9.3 Hz, 2H), 6.70 (dd, *J* = 9.4, 4.3 Hz, 2H), 6.99 (t, *J* = 8.8 Hz, 2H); <sup>13</sup>C NMR (126 MHz, chloroform-*d*) δ ppm 24.99 (CH<sub>2</sub> cyclobutane), 37.52 (CH cyclobutane), 56.66 (N-CH<sub>2</sub>), 114.47, 114.52 (d, Ar-CH), 115.33, 115.51 (d, Ar-CH), 146.43, 146.45 (d, Hz, Ar-C), 156.54, 154.67 (d,

Ar-CF).  $^{19}\text{F}$  NMR (376 MHz, chloroform-*d*)  $\delta$  ppm -130.39 (m, 1 F); **HRMS** (ESI) Calc. for  $[\text{C}_{12}\text{H}_{14}\text{FN}]^+$  = 191.1110, Found = 191.1038.

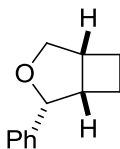


**Table 1, entry 6:**  $^1\text{H}$  NMR (500 MHz, benzene-*d*<sub>6</sub>)  $\delta$  ppm 1.58 - 1.66 (m, 1 H) 1.77 - 1.85 (m, 1 H) 1.86 - 1.95 (m, 1 H) 1.95 - 2.04 (m, 1 H) 2.49 - 2.57 (m, 1 H) 2.82 - 2.89 (m, 1 H) 3.69 (dd,  $J=9.10, 1.80$  Hz, 1 H, OCH<sub>2</sub>) 3.74 (dd,  $J=9.10, 6.00$  Hz, 1 H, OCH<sub>2</sub>) 4.92 (s, 1 H, OC-H) 7.04 - 7.09 (m, 1 H, Ar-H) 7.14 - 7.19 (m, 2 H, Ar-H) 7.24 (s, 2 H, Ar-H);  $^{13}\text{C}$  NMR (126 MHz, chloroform-*d*)  $\delta$  ppm 23.90, 24.04, 39.41, 45.03, 73.70, 86.68, 125.76, 126.93, 128.26, 142.23; **HRMS** (GC-MS) Calc. for  $[\text{C}_{12}\text{H}_{13}\text{O}]^+$  = 174.1045, Found = 174.1030.

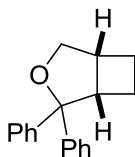
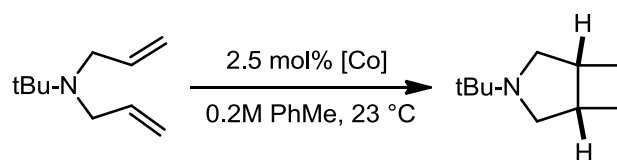


**Table 1, entry 7:**  $^1\text{H}$  NMR (501 MHz, benzene-*d*<sub>6</sub>)  $\delta$  ppm 1.42 - 1.50 (m, 1 H) 1.67 - 1.76 (m, 1 H) 1.76 - 1.85 (m, 1 H) 1.87 - 1.97 (m, 1 H) 2.45 - 2.52 (m, 1 H) 3.54 - 3.60 (m, 1 H) 3.63 (dd,  $J=9.14, 6.31$  Hz, 1 H) 3.76 (d,  $J=9.46$  Hz, 1 H) 6.96 - 7.02 (m, 2 H) 7.09 - 7.14 (m, 4 H) 7.45 (dd,  $J=8.20, 0.95$  Hz, 2 H) 7.54 (dd,  $J=8.04, 1.10$  Hz, 2 H);  $^{13}\text{C}$  NMR (126 MHz, benzene-*d*<sub>6</sub>)  $\delta$  ppm 21.63 (cyclobutane CH<sub>2</sub>), 24.20 (cyclobutane CH<sub>2</sub>), 39.55 (cyclobutane CH), 45.96 (cyclobutane CH), 73.18 (O-CH<sub>2</sub>), 90.99 (O-CPh<sub>2</sub>), 126.88 (Ar-CH), 126.95 (Ar-CH), 127.01 (Ar-CH), 127.42 (Ar-CH), 128.65 (Ar-CH), 128.95 (Ar-CH), 144.95 (Ar-CH), 145.79 (Ar-CH); **HRMS** (GC-MS) Calc. for  $[\text{C}_{18}\text{H}_{18}\text{O}]^+$  = 250.1358, Found = 250.1347.

**Table S1.** *N,N*-diallyl-*tert*-butylamine catalyst effects.



entry	[Co]	time (h) <sup>a</sup>
1	( <sup>i</sup> PrPDI)CoN <sub>2</sub> ( <b>1</b> )	3
2	( <sup>Tri</sup> cPDI)CoN <sub>2</sub> ( <b>2</b> )	<0.1
3	( <sup>Me</sup> PDI)CoN <sub>2</sub> ( <b>4</b> )	1
4	( <sup>i</sup> PrEtPDI)CoN <sub>2</sub> ( <b>5</b> )	15 <sup>b</sup>
5	( <sup>i</sup> Pr <sup>i</sup> PrPDI)CoN <sub>2</sub> ( <b>6</b> )	NR
6	4-pyrr-( <sup>i</sup> PrPDI)CoN <sub>2</sub> ( <b>7</b> )	15

<sup>a</sup>Time to >98% conversion. <sup>b</sup>41% conversion.

NR = no reaction

## II. Additional X-ray Crystallographic Data.

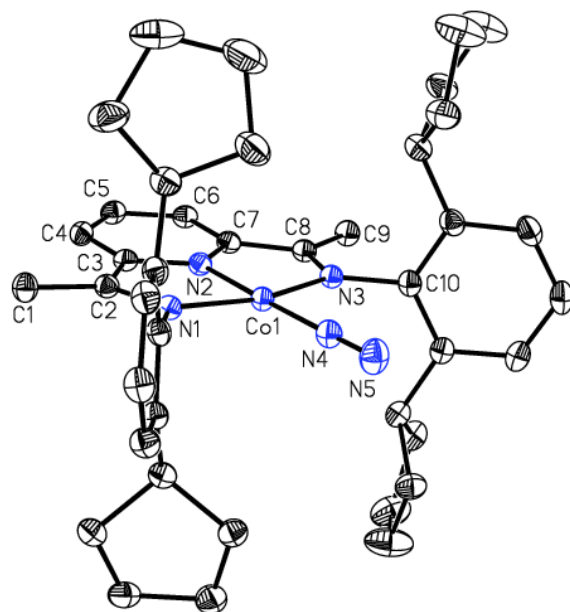


**Figure S1.** Molecular structure of  $(C^{5H9}PDI)CoN_2$  at 30% probability ellipsoids. Hydrogen atoms omitted for clarity.

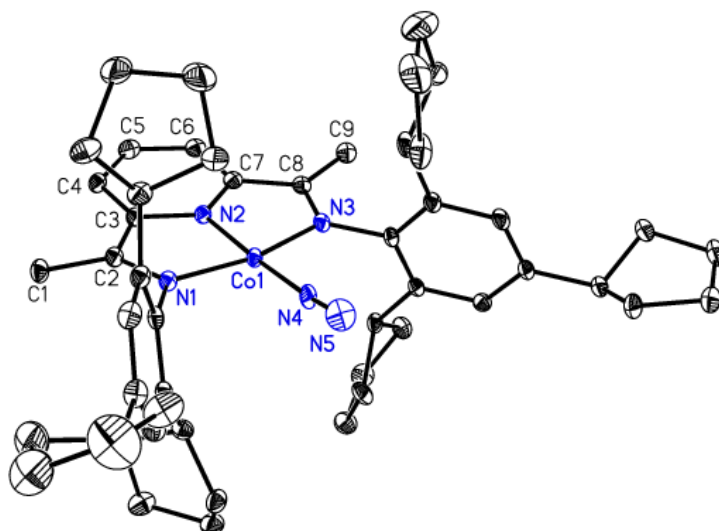


**Figure S2.** Molecular structure of **2** at 30% probability ellipsoids. Hydrogen atoms omitted for clarity.

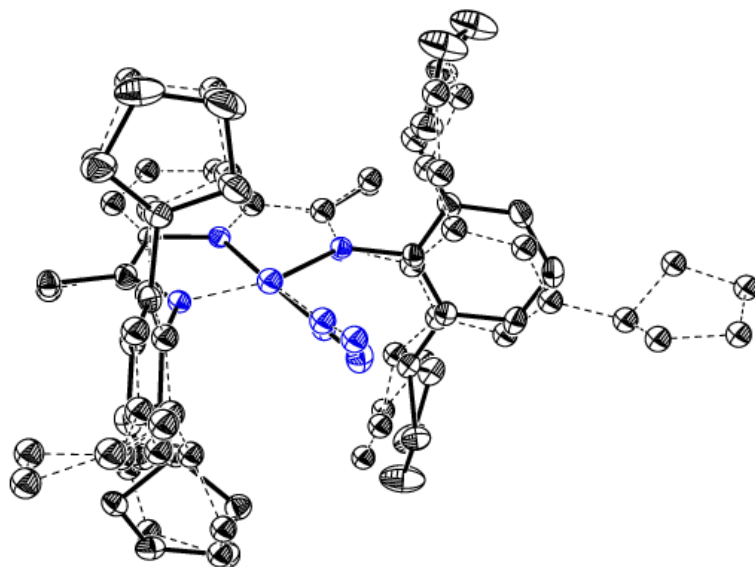


**Figure S3.** Overlay of  $(^{C5H9}PDI)CoN_2$  and **2** at 30% probability ellipsoids. Hydrogen atoms omitted for clarity.

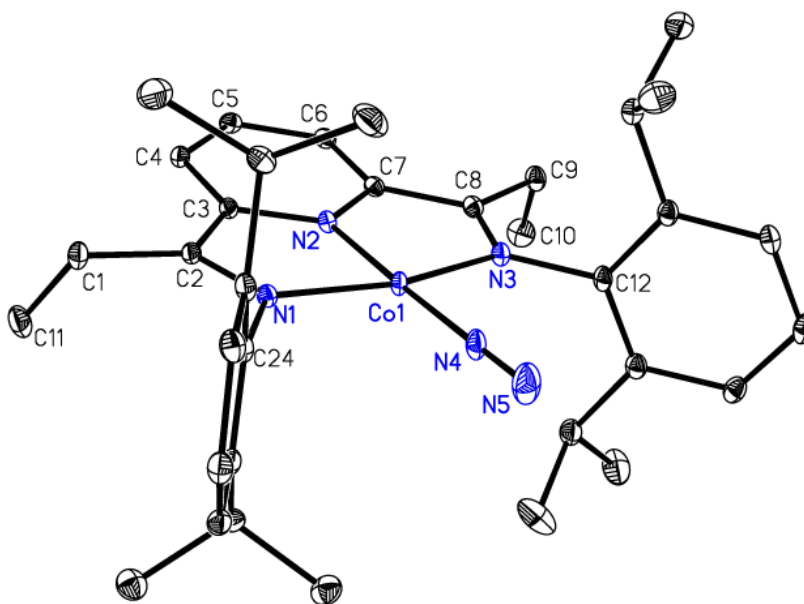


**Figure S4.** Molecular structure of **5** at 30% probability ellipsoids. Hydrogen atoms omitted for clarity.

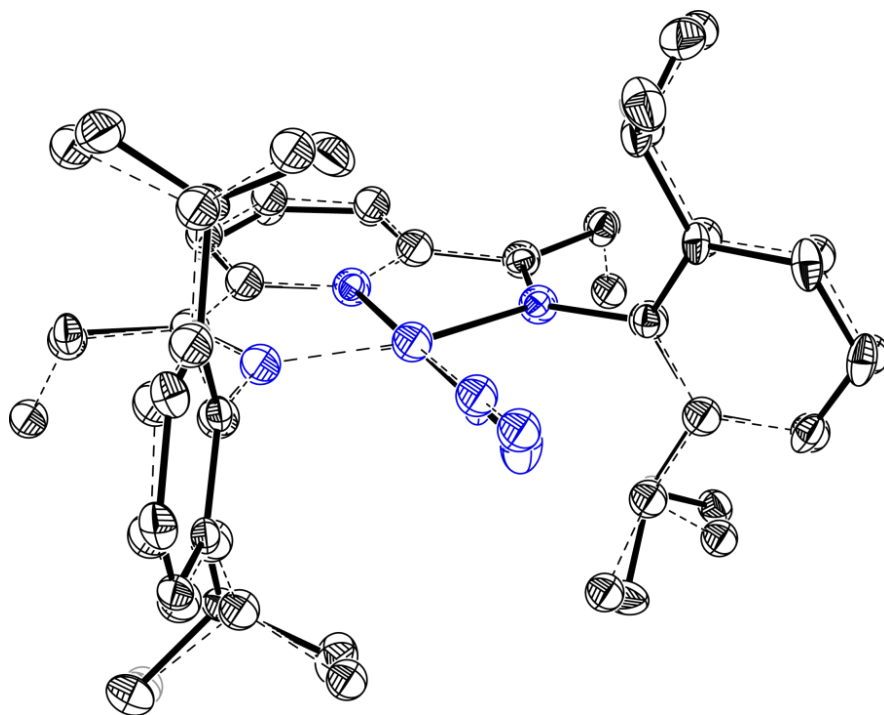


**Figure S5.** Overlay of **1** and **5** at 30% probability ellipsoids. Hydrogen atoms omitted for clarity.

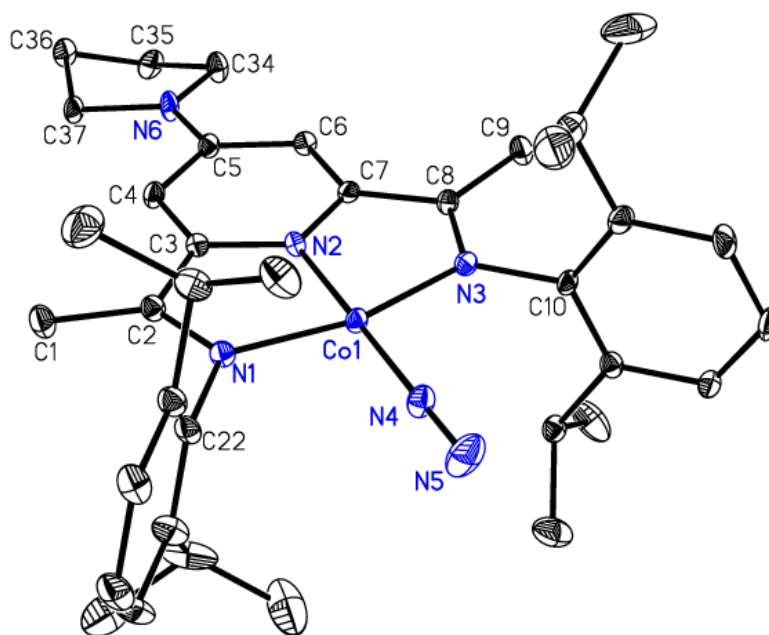


**Figure S6.** Molecular structure of **7** at 30% probability ellipsoids. Hydrogen atoms omitted for clarity.



**Table S2.** Selected bond distances (Å) for **1**, (<sup>C5H9</sup>PDI)CoN<sub>2</sub>, **5**, and **7**.

	<b>1</b> <sup>2</sup>	( <sup>C5H9</sup> PDI)CoN <sub>2</sub>	<b>2</b>	<b>5</b>	<b>7</b>
Co – N(1)	1.882(2)	1.8773(14)	1.875(2)	1.8918(11)	1.879(3)
Co – N(3)	1.881(2)	1.8719(15)	1.870(2)	1.8911(10)	1.872(3)
Co – N(2)	1.816(2)	1.8084(14)	1.808(2)	1.8179(10)	1.818(2)
Co – N(4)	1.787(2)	1.7884(16)	1.789(2)	1.7877(11)	1.770(3)
N(4) – N(5)	1.114(3)	1.104(2)	1.068(4)	1.1087(17)	1.111(4)
N(1) – C(2)	1.343(3)	1.332(2)	1.335(3)	1.3406(16)	1.350(4)
N(3) – C(8)	1.338(3)	1.341(2)	1.343(3)	1.3403(16)	1.345(4)
C(2) – C(3)	1.433(4)	1.429(2)	1.435(4)	1.4366(17)	1.442(4)
C(3) – N(2)	1.436(4)	1.418(2)	1.371(3)	1.3694(15)	1.368(4)

**X-ray Crystallographic Experimental Details for (<sup>C5H9</sup>PDI)CoN<sub>2</sub>**

## Crystal Data

C <sub>41</sub> H <sub>51</sub> CoN <sub>5</sub>	Z = 2
M <sub>r</sub> = 672.80	F(000) = 718
Triclinic, P <sup>-</sup> 1	D <sub>x</sub> = 1.173 Mg m <sup>-3</sup>
a = 12.5215 (3) Å	Cu Kα radiation, λ = 1.54178 Å
b = 13.1868 (3) Å	Cell parameters from 9825 reflections
c = 14.6751 (3) Å	θ = 3.9–66.6°
α = 88.510 (1)°	μ = 3.78 mm <sup>-1</sup>
β = 65.856 (1)°	T = 100 K
γ = 61.762 (1)°	Shard, green
V = 1905.24 (7) Å <sup>3</sup>	0.12 × 0.08 × 0.07 mm

## Data collection

Radiation source: fine-focus sealed tube	6316 reflections with I > 2σ(I)
graphite	R <sub>int</sub> = 0.0000
Absorption correction: multi-scan SADABS v2008/1 (Bruker AXS)	θ <sub>max</sub> = 66.7°, θ <sub>min</sub> = 3.9°
T <sub>min</sub> = 0.597, T <sub>max</sub> = 0.753	h = -13→14
6749 measured reflections	k = -15→15
6749 independent reflections	l = 0→17

## Refinement

Refinement on $F^2$	Primary atom site location: structure-invariant direct methods
Least-squares matrix: full	Secondary atom site location: difference Fourier map
$R[F^2 > 2\sigma(F^2)] = 0.049$	Hydrogen site location: inferred from neighbouring sites
$wR(F^2) = 0.131$	H-atom parameters constrained
$S = 1.10$	$w = 1/[\sigma^2(F_o^2) + (0.0592P)^2 + 1.6047P]$ where $P = (F_o^2 + 2F_c^2)/3$
6749 reflections	$(\Delta/\sigma)_{\max} = 0.016$
420 parameters	$\Delta_{\max} = 1.01 \text{ e } \text{\AA}^{-3}$
0 restraints	$\Delta_{\min} = -0.71 \text{ e } \text{\AA}^{-3}$

## X-ray Crystallographic Experimental Details for 2

### Crystal data

$\text{C}_{51}\text{H}_{67}\text{CoN}_5$	$F(000) = 1740$
$M_r = 809.02$	$D_x = 1.108 \text{ Mg m}^{-3}$
Monoclinic, $P2_1/c$	Cu $K\alpha$ radiation, $\lambda = 1.54178 \text{ \AA}$
$a = 16.6004 (5) \text{ \AA}$	Cell parameters from 9874 reflections
$b = 26.8286 (8) \text{ \AA}$	$\theta = 3.3\text{--}66.7^\circ$
$c = 11.5360 (3) \text{ \AA}$	$\mu = 3.04 \text{ mm}^{-1}$
$\beta = 109.228 (2)^\circ$	$T = 100 \text{ K}$
$V = 4851.1 (2) \text{ \AA}^3$	Shard, black
$Z = 4$	$0.25 \times 0.11 \times 0.08 \text{ mm}$

### Data collection

Bruker APEX-II CCD diffractometer	6657 reflections with $I > 2\sigma(I)$
$\phi$ and $\omega$ scans	$R_{\text{int}} = 0.045$
Absorption correction: multi-scan SADABS v21014/5 (BRUKER AXS)	$\theta_{\max} = 66.8^\circ$ , $\theta_{\min} = 2.8^\circ$
$T_{\min} = 0.598$ , $T_{\max} = 0.753$	$h = -19 \rightarrow 19$
29075 measured reflections	$k = -24 \rightarrow 31$
8484 independent reflections	$l = -13 \rightarrow 13$

## Refinement

Refinement on $F^2$	0 restraints
Least-squares matrix: full	Hydrogen site location: inferred from neighbouring sites
$R[F^2 > 2\sigma(F^2)] = 0.052$	H-atom parameters constrained
$wR(F^2) = 0.131$	$w = 1/[\sigma^2(F_o^2) + (0.0585P)^2 + 2.9944P]$ where $P = (F_o^2 + 2F_c^2)/3$
$S = 1.04$	$(\Delta/\sigma)_{\max} = 0.001$
8484 reflections	$\Delta)_{\max} = 0.53 \text{ e } \text{\AA}^{-3}$
516 parameters	$\Delta)_{\min} = -0.33 \text{ e } \text{\AA}^{-3}$

## X-ray Crystallographic Experimental Details for 5

## Crystal data

$C_{35}H_{47}CoN_5$	$F(000) = 1276$
$M_r = 596.70$	$D_x = 1.237 \text{ Mg m}^{-3}$
Monoclinic, $P2_1/c$	Cu $K\alpha$ radiation, $\lambda = 1.54178 \text{ \AA}$
$a = 11.7099 (2) \text{ \AA}$	Cell parameters from 9753 reflections
$b = 13.5494 (2) \text{ \AA}$	$\theta = 3.9\text{--}72.2^\circ$
$c = 21.0167 (4) \text{ \AA}$	$\mu = 4.42 \text{ mm}^{-1}$
$\beta = 106.020 (1)^\circ$	$T = 100 \text{ K}$
$V = 3205.06 (10) \text{ \AA}^3$	Block
$Z = 4$	$0.06 \times 0.06 \times 0.02 \text{ mm}$

## Data collection

Bruker APEX-II CCD diffractometer	6044 reflections with $I > 2\sigma(I)$
$\phi$ and $\omega$ scans	$R_{\text{int}} = 0.031$
Absorption correction: multi-scan SADABS v2014/2 (Bruker AXS)	$\theta_{\max} = 72.3^\circ$ , $\theta_{\min} = 3.9^\circ$
$T_{\min} = 0.680$ , $T_{\max} = 0.754$	$h = -14 \rightarrow 14$
58696 measured reflections	$k = -15 \rightarrow 16$
6314 independent reflections	$l = -25 \rightarrow 25$

## Refinement

Refinement on $F^2$	0 restraints
Least-squares matrix: full	Hydrogen site location: inferred from neighbouring sites
$R[F^2 > 2\sigma(F^2)] = 0.029$	H-atom parameters constrained
$wR(F^2) = 0.076$	$w = 1/[\sigma^2(F_o^2) + (0.0435P)^2 + 1.1461P]$ where $P = (F_o^2 + 2F_c^2)/3$
$S = 1.05$	$(\Delta/\sigma)_{\max} = 0.003$
6314 reflections	$\Delta)_{\max} = 0.34 \text{ e } \text{\AA}^{-3}$
380 parameters	$\Delta)_{\min} = -0.16 \text{ e } \text{\AA}^{-3}$

## X-ray Crystallographic Experimental Details for 7

## Crystal data

$C_{41}H_{55}CoN_6$	$F(000) = 1480$
$M_r = 690.84$	$D_x = 1.051 \text{ Mg m}^{-3}$
Monoclinic, $P2_1/n$	Cu $K\alpha$ radiation, $\lambda = 1.54178 \text{ \AA}$
$a = 16.1752 (5) \text{ \AA}$	Cell parameters from 9688 reflections
$b = 15.4059 (5) \text{ \AA}$	$\theta = 4.0\text{--}66.7^\circ$
$c = 17.8232 (5) \text{ \AA}$	$\mu = 3.31 \text{ mm}^{-1}$
$\beta = 100.562 (2)^\circ$	$T = 100 \text{ K}$
$V = 4366.2 (2) \text{ \AA}^3$	Irregular, brown
$Z = 4$	$0.18 \times 0.06 \times 0.04 \text{ mm}$

## Data collection

Bruker APEX-II CCD diffractometer	6493 reflections with $I > 2\sigma(I)$
$\phi$ and $\omega$ scans	$R_{\text{int}} = 0.058$
Absorption correction: multi-scan SADABS v2014/2 (Bruker AXS)	$\theta_{\max} = 66.9^\circ$ , $\theta_{\min} = 3.4^\circ$
$T_{\min} = 0.499$ , $T_{\max} = 0.753$	$h = -19 \rightarrow 19$
42248 measured reflections	$k = -18 \rightarrow 18$
7684 independent reflections	$l = -21 \rightarrow 21$

## Refinement

Refinement on $F^2$	0 restraints
Least-squares matrix: full	Hydrogen site location: inferred from neighbouring sites
$R[F^2 > 2\sigma(F^2)] = 0.065$	H-atom parameters constrained
$wR(F^2) = 0.149$	$w = 1/[\sigma^2(F_o^2) + (0.0362P)^2 + 9.6007P]$ where $P = (F_o^2 + 2F_c^2)/3$
$S = 1.10$	$(\Delta/\sigma)_{\max} = 0.001$
7684 reflections	$\Delta_{\max} = 0.63 \text{ e } \text{\AA}^{-3}$
444 parameters	$\Delta_{\min} = -0.63 \text{ e } \text{\AA}^{-3}$

## X-ray Crystallographic Experimental Details for 8

## Crystal data

$\text{C}_{50}\text{H}_{64}\text{CoN}_4\text{O}$	$D_x = 1.021 \text{ Mg m}^{-3}$
$M_r = 795.98$	Cu $K\alpha$ radiation, $\lambda = 1.54178 \text{ \AA}$
Orthorhombic, $Pbcn$	Cell parameters from 9661 reflections
$a = 16.0184 (7) \text{ \AA}$	$\theta = 3.6\text{--}66.8^\circ$
$b = 19.8059 (8) \text{ \AA}$	$\mu = 2.85 \text{ mm}^{-1}$
$c = 32.6528 (14) \text{ \AA}$	$T = 100 \text{ K}$
$V = 10359.4 (8) \text{ \AA}^3$	Block, black
$Z = 8$	$0.08 \times 0.08 \times 0.03 \text{ mm}$
$F(000) = 3416$	

## Data collection

Absorption correction: multi-scan <i>SADABS</i> v2008/1 (Bruker AXS)	$R_{\text{int}} = 0.112$
$T_{\min} = 0.525, T_{\max} = 0.753$	$\theta_{\max} = 66.8^\circ, \theta_{\min} = 2.7^\circ$
135177 measured reflections	$h = -19 \rightarrow 19$
9189 independent reflections	$k = -23 \rightarrow 23$
7194 reflections with $I > 2\sigma(I)$	$l = -38 \rightarrow 38$

## Refinement

Refinement on $F^2$	4 restraints
---------------------	--------------

Least-squares matrix: full	Hydrogen site location: mixed
$R[F^2 > 2\sigma(F^2)] = 0.079$	H atoms treated by a mixture of independent and constrained refinement
$wR(F^2) = 0.203$	$w = 1/[\sigma^2(F_o^2) + (0.0923P)^2 + 15.7044P]$ where $P = (F_o^2 + 2F_c^2)/3$
$S = 1.10$	$(\Delta/\sigma)_{\max} = 0.001$
9189 reflections	$\Delta_{\max} = 0.74 \text{ e } \text{\AA}^{-3}$
526 parameters	$\Delta_{\min} = -0.68 \text{ e } \text{\AA}^{-3}$

**Table S3.** Selected bond distances (Å) and angles (deg) of **8**.

<b>8</b>	
Co(1)-N(1)	2.152(3)
Co(1)-N(2)	1.901(3)
Co(1)-N(3)	2.567(3)
Co(1)-C(38)	2.050(4)
Co(1)-C(43)	2.055(3)
N(1)-C(2)	1.298(5)
N(3)-C(8)	1.289(4)
C(2)-C(3)	1.452(5)
C(7)-C(8)	1.475(5)
C(38)-C(39)	1.388(5)
C(39)-C(42)	2.673(5)
C(42)-C(43)	1.393(5)
N(1)-Co(1)-N(2)	80.0(1)
N(1)-Co(1)-N(3)	153.1(1)
N(2)-Co(1)-N(3)	73.3(1)
C(38)-Co(1)-C(43)	154.3(1)
C(38)-Co(1)-N(1)	98.1(1)
C(38)-Co(1)-N(2)	98.7(1)
C(38)-Co(1)-N(3)	89.2(1)
C(43)-Co(1)-N(1)	96.5(1)
C(43)-Co(1)-N(2)	104.5(1)
C(43)-Co(1)-N(3)	87.1(1)

### III. Electrochemical Data

**Data collection.** Cyclic voltammograms (CVs) were collected in THF solution (1 mM in compound) with  $[n\text{Bu}_4\text{N}][\text{PF}_6]$  (0.1M), using a 3 mm glassy-carbon working electrode, platinum wire as the counter electrode, and silver wire as the reference in a drybox equipped with electrochemical outlets. CVs were recorded using a BASi EC Epsilon-EC software. All CVs were run at a scan rate of 100 mV/s at 295 K. Potentials are reported versus ferrocene/ferrocenium and were obtained using the in situ method.

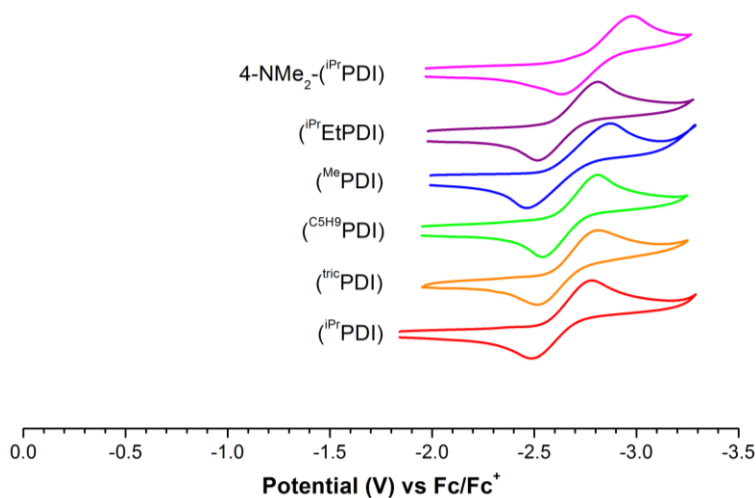


**Figure S7.** Cyclic voltammograms for free bis(imino)pyridine ligands used in this study.

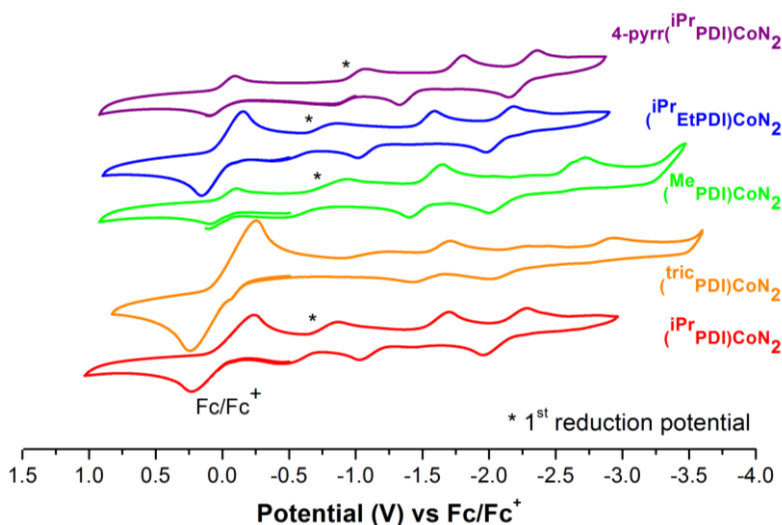


**Figure S8.** Cyclic voltammograms for bis(imino)pyridine cobalt dinitrogen compounds used in this study.

#### IV. Additional EPR Spectroscopic Data

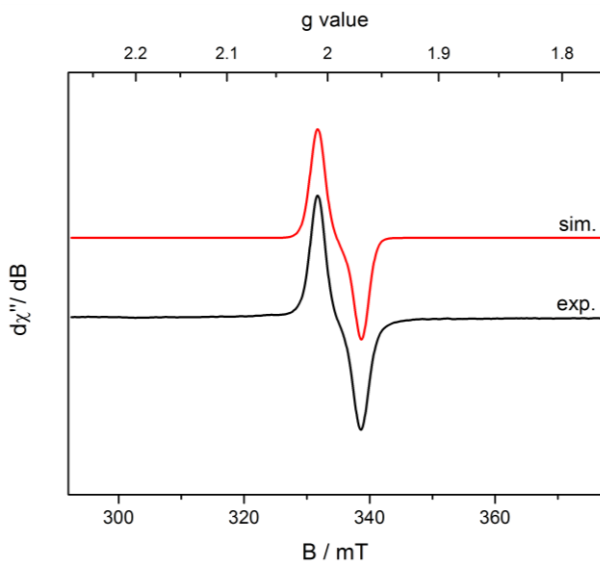


**Figure S9.** Toluene solution X-band EPR spectra of **1** was recorded at 295 K (microwave frequency = 9.759 GHz, power = 0.63 mW, modulation amplitude = 4.0 mT/100 kHz).

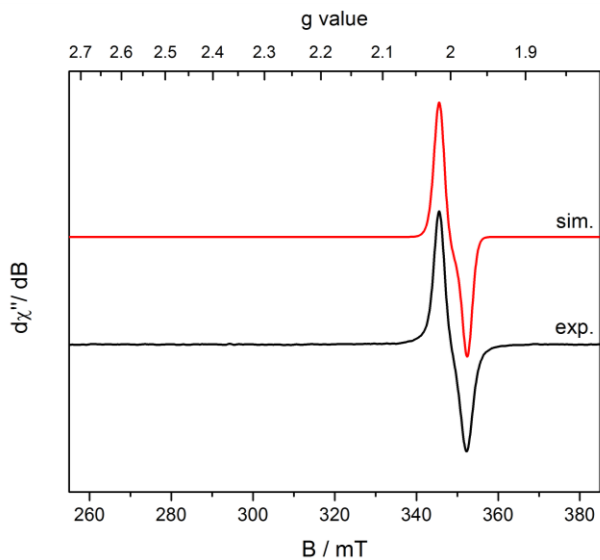


**Figure S10.** Toluene solution X-band EPR spectra of **2** was recorded at 295 K (microwave frequency = 9.759 GHz, power = 0.63 mW, modulation amplitude = 4.0 mT/100 kHz).



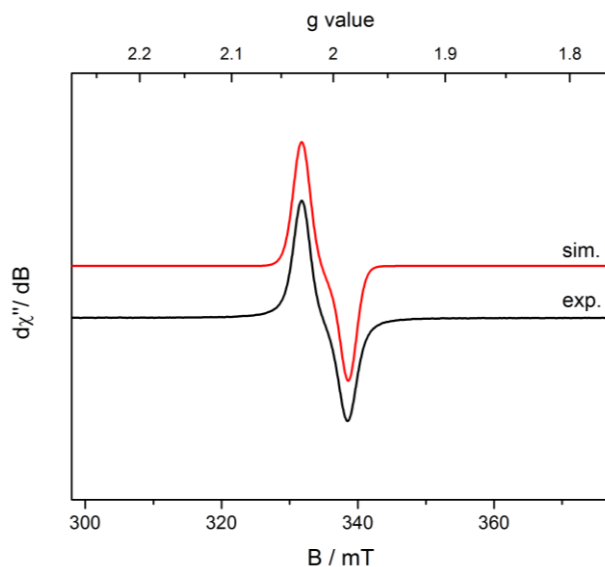


**Figure S11.** Toluene solution X-band EPR spectra of  $(^{55}\text{Co})\text{PDI}(\text{C}_5\text{H}_9)_2$  was recorded at 295 K (microwave frequency = 9.759 GHz, power = 0.63 mW, modulation amplitude = 4.0 mT/100 kHz).

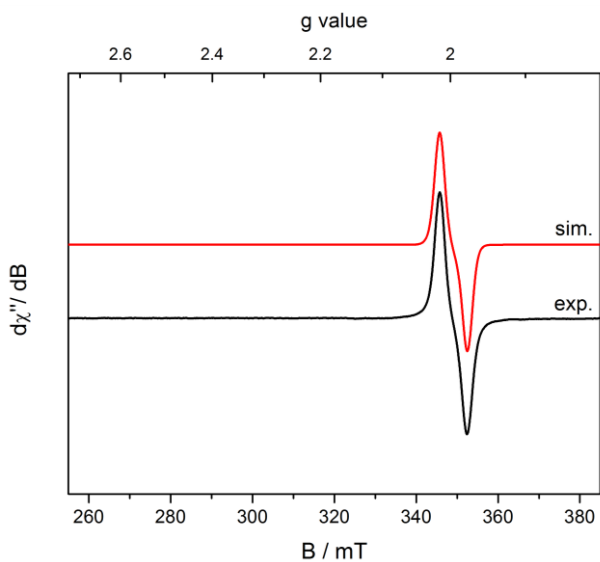


**Figure S12.** Toluene solution X-band EPR spectra of **3** was recorded at 295 K (microwave frequency = 9.759 GHz, power = 0.63 mW, modulation amplitude = 4.0 mT/100 kHz).

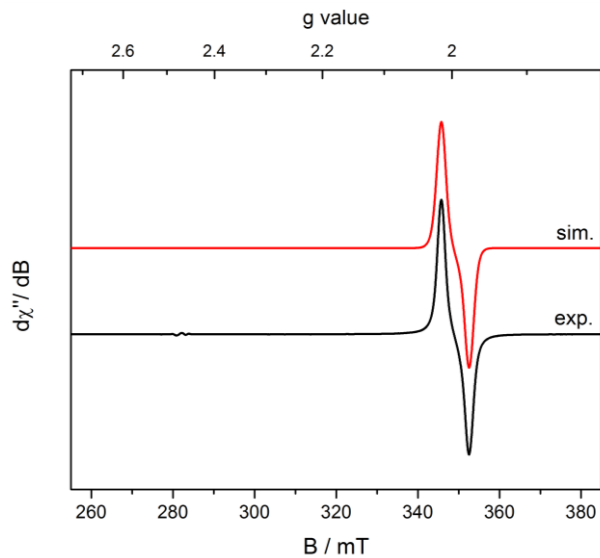


**Figure S13.** Toluene solution X-band EPR spectra of **4** was recorded at 295 K (microwave frequency = 9.759 GHz, power = 0.63 mW, modulation amplitude = 4.0 mT/100 kHz).

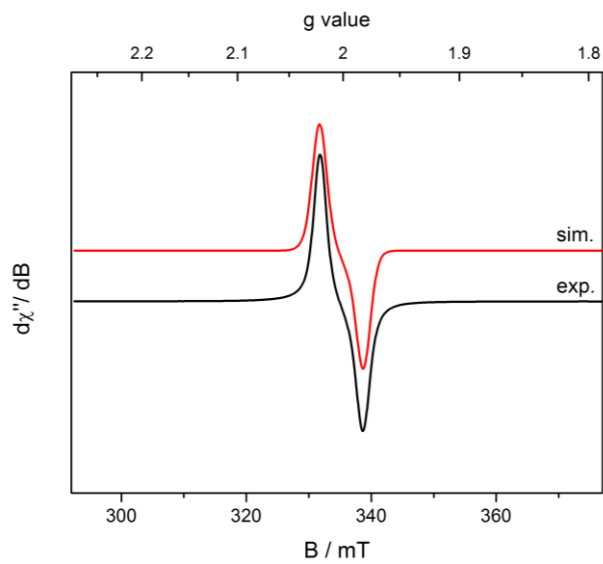


**Figure S14.** Toluene solution X-band EPR spectra of **5** was recorded at 295 K (microwave frequency = 9.374 GHz, power = 0.63 mW, modulation amplitude = 4.0 mT/100 kHz).

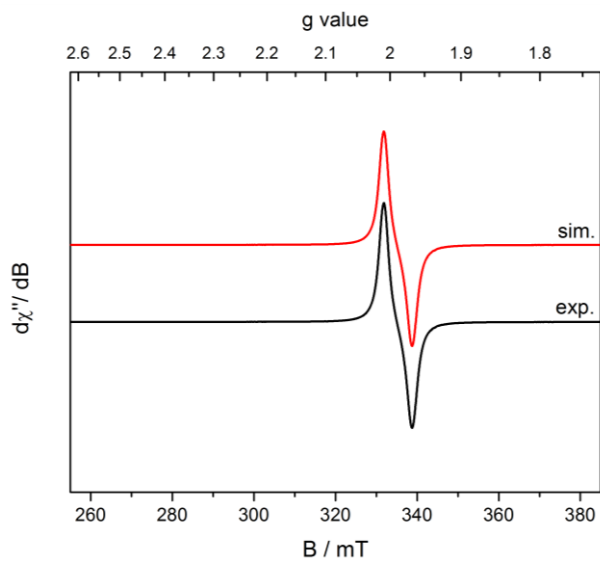


**Figure S15.** Toluene solution X-band EPR spectra of **6** was recorded at 295 K (microwave frequency = 9.374 GHz, power = 0.63 mW, modulation amplitude = 4.0 mT/100 kHz).

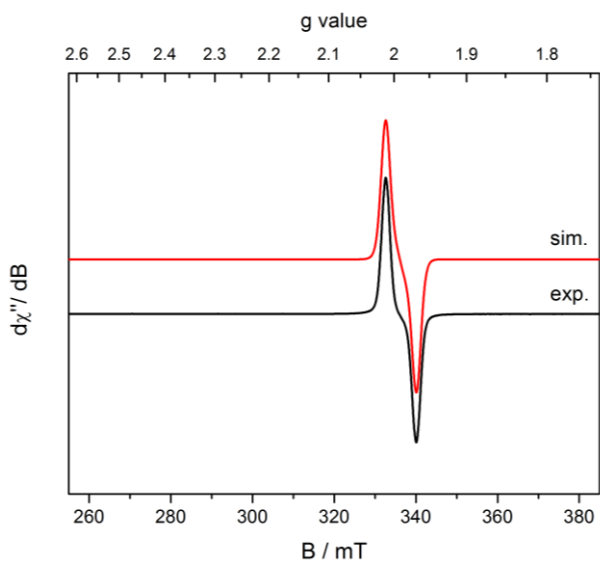


**Figure S16.** Toluene solution X-band EPR spectra of **7** was recorded at 295 K (microwave frequency = 9.379 GHz, power = 0.63 mW, modulation amplitude = 4.0 mT/100 kHz).

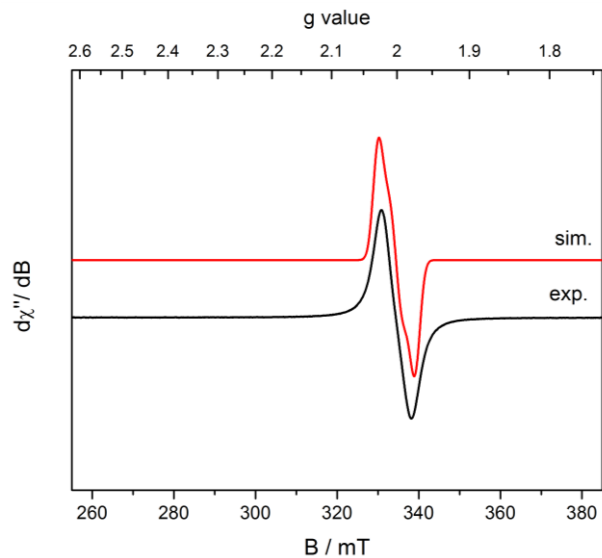


**Figure S17.** Toluene solution X-band EPR spectra of  $(i\text{Pr}^{\text{TBPDI}})\text{CoN}_2$  was recorded at 295 K (microwave frequency = 9.374 GHz, power = 0.63 mW, modulation amplitude = 4.0 mT/100 kHz).

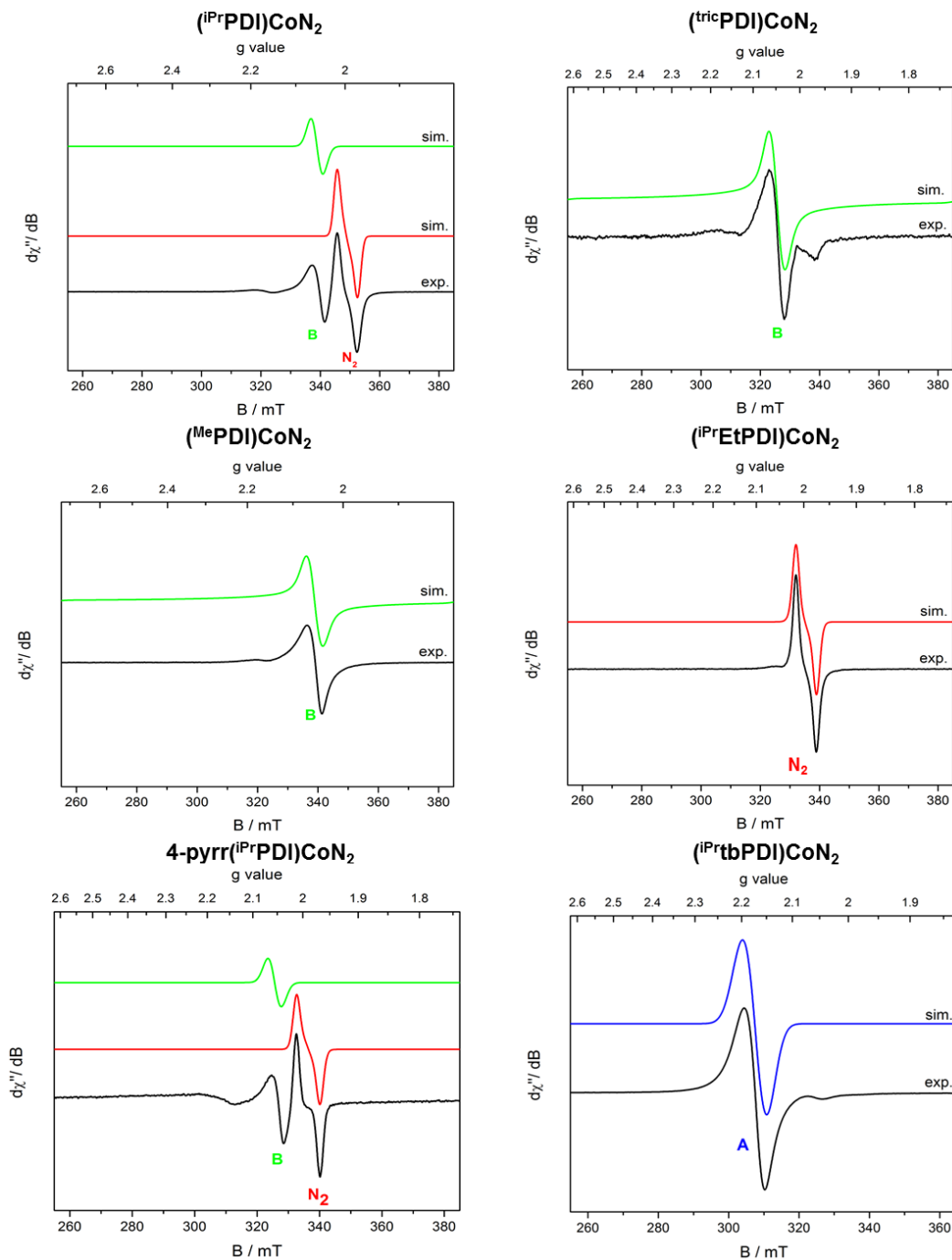


**Figure S18.** Toluene solution X-band EPR spectra of mixtures of 40 equiv *N,N*-diallyl-4-fluoroaniline with the specified (PDI)CoN<sub>2</sub>. 100 equiv used with (<sup>Tric</sup>PDI)CoN<sub>2</sub>. All EPR spectra were recorded at 295 K (microwave frequency = 9.374 GHz, power = 0.63 mW, modulation amplitude = 4.0 mT/100 kHz). Mixtures with (<sup>i</sup>PrPDI)CoN<sub>2</sub> and (<sup>Me</sup>PDI)CoN<sub>2</sub> microwave frequency = 9.759.

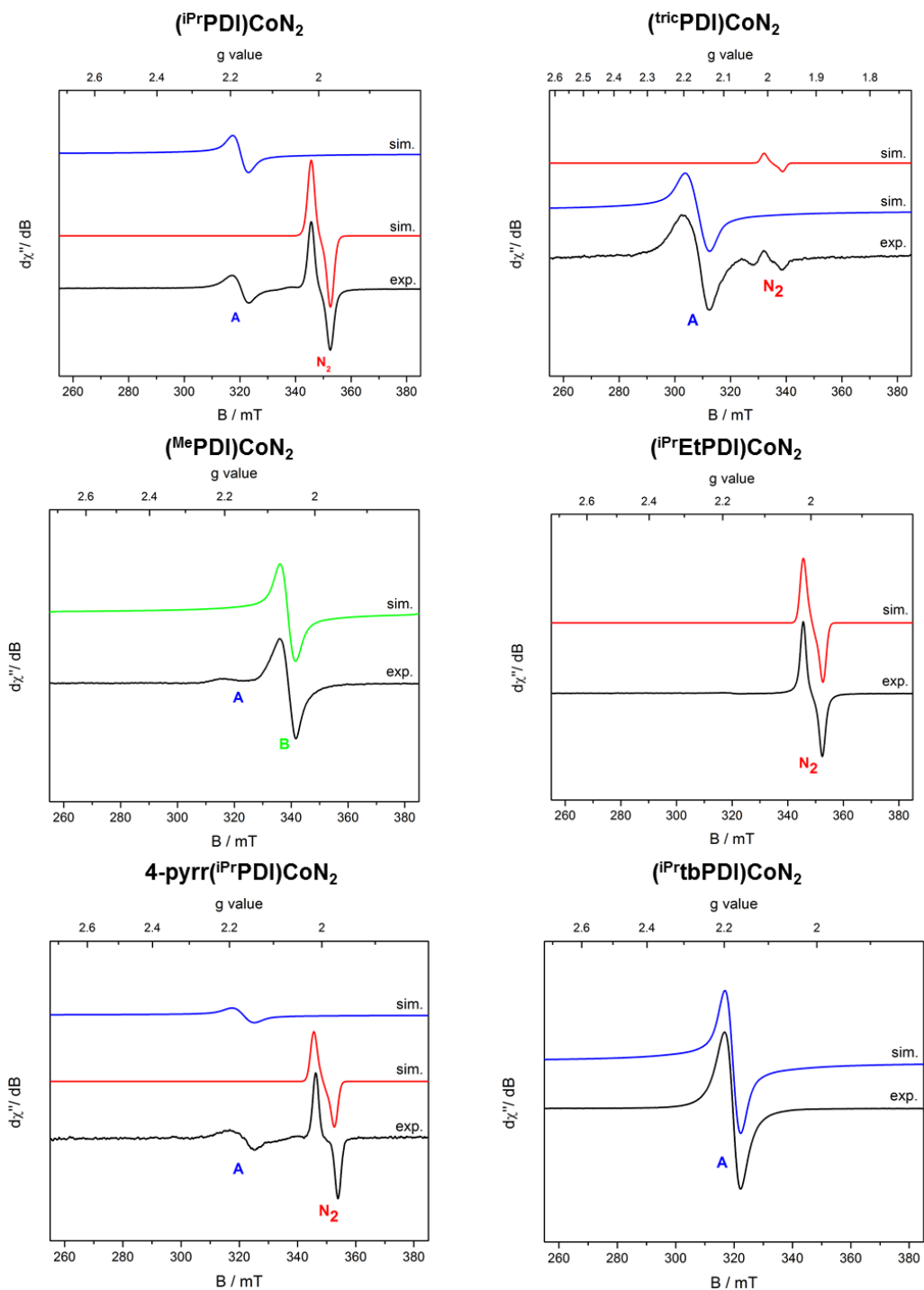


**Figure S19.** Toluene solution X-band EPR spectra of mixtures of 40 equiv *N,N*-diallyl-*tert*-butylamine with the specified Co-compounds. 100 equiv used with (<sup>Tricy</sup>PDI)CoN<sub>2</sub>. All EPR spectra were recorded at 295 K (microwave frequency = 9.759 GHz, power = 0.63 mW, modulation amplitude = 4.0 mT/100 kHz). Mixture with (<sup>Tricy</sup>EtPDI)CoN<sub>2</sub> microwave frequency = 9.374.

## V. Additional Kinetic Data

*Procedure for kinetic experiments reaction of (<sup>iPr</sup>PDI)CoN<sub>2</sub> (1) with N,N-diallyl-4-fluoroaniline (Figure S20)* : A stock solution of **1** (20 mg, 0.035 mmol) in PhMe (1.53 g) was prepared and evenly distributed by mass into 3 separate vials. N,N-diallyl-4-fluoroaniline (22 mg, 0.012 mmol) was added via microsyringe to each vial and sealed at 23 °C. Aliquots (15 μL) were taken at the designated time points, diluted with Et<sub>2</sub>O (1 mL) and analyzed by GC until at least two half-lives were reached. This procedure was repeated twice more at 5, and 2.5 mol% **1** adjusting the amounts of substrate and PhMe used so that the concentration of substrate is 0.2M. Errors bars indicate one standard deviation from the mean.

Experiment with 2.5 mol% **1**: the data fit to an exponential decay to the equation  $y = 0.20e^{-0.000037x}$ ,  $R^2 = 0.9991$  (left graph). Plotting the  $\ln[\text{N,N-diallyl-4-fluoroaniline}]$  versus time, the data fit to a linear decay to the equation  $y = -0.00004x - 1.59$ ,  $R^2 = 0.9991$  (right graph).

Experiment with 5 mol% **1**: the data fit to an exponential decay to the equation  $y = 0.22e^{-0.000091x}$ ,  $R^2 = 0.9863$  (left graph). Plotting the  $\ln[\text{N,N-diallyl-4-fluoroaniline}]$  versus time, the data fit to a linear decay to the equation  $y = -0.00008x - 1.51$ ,  $R^2 = 0.9880$  (right graph).

Experiment with 10 mol% **1**: the data fit to an exponential decay to the equation  $y = 0.22e^{-0.00021x}$ ,  $R^2 = 0.9910$  (left graph). Plotting the  $\ln[\text{N,N-diallyl-4-fluoroaniline}]$  versus time, the data fit to a linear decay to the equation  $y = -0.00021x - 1.51$ ,  $R^2 = 0.9910$  (right graph).

The observed rates obtained from these experiments were plotted against the concentration of **1**, and fitted to a line described by the equation  $y = 0.012x - 0.000023$ ,  $R^2 = 0.9994$  (bottom graph).

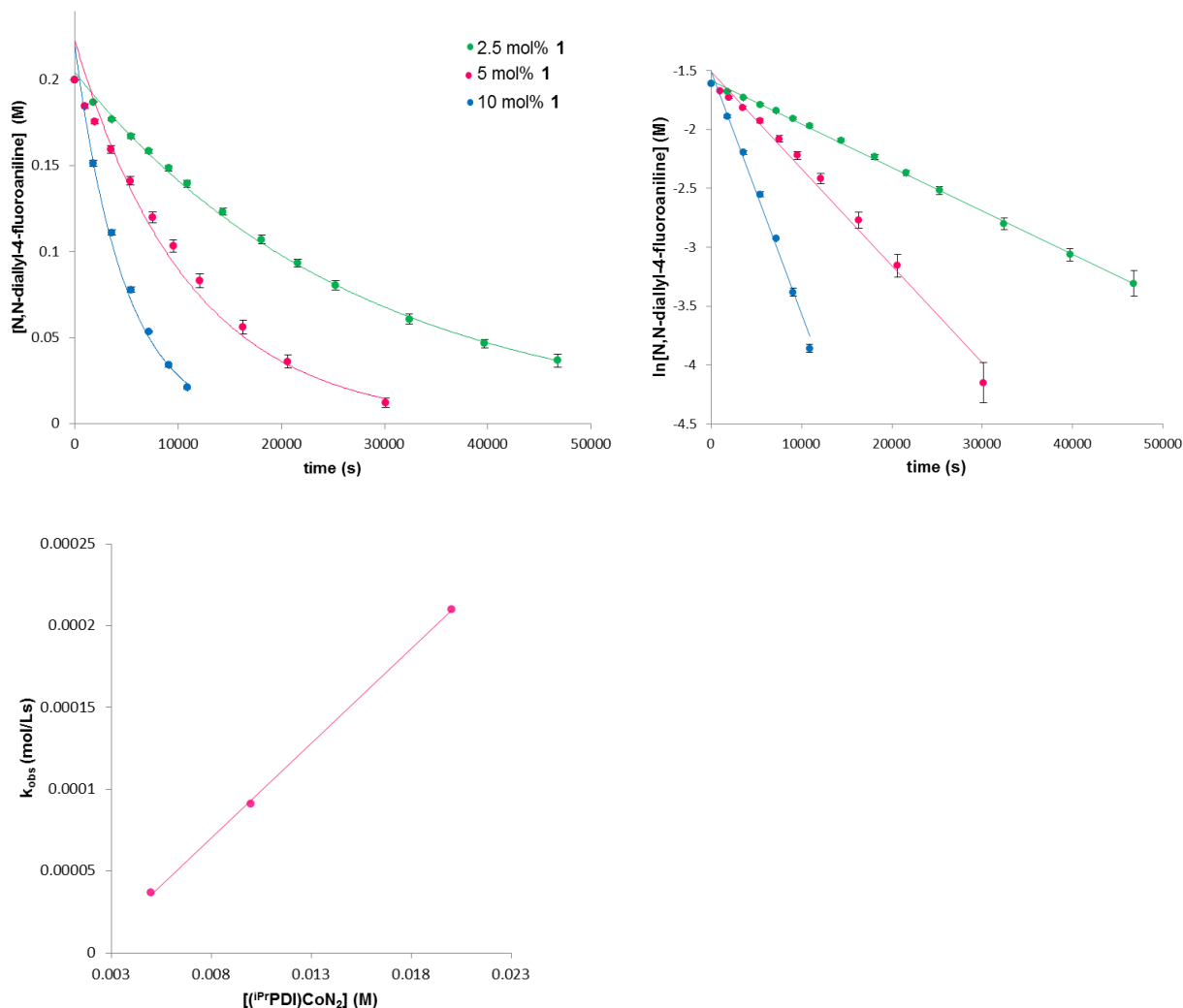


**Figure S20.** Kinetic plots for the cycloaddition of *N,N*-diallyl-4-fluoroaniline in the presence of **1**. *Procedure for kinetic experiments reaction of  $(^{iPr}PDI)CoN_2$  (**1**) with *N,N*-diallyl-*tert*-butylamine (Figure S21):* A stock solution of **1** (20 mg, 0.035 mmol) in PhMe (3.05 g) was prepared and evenly distributed by mass into 3 separate vials. *N,N*-diallyl-*tert*-butylamine (36 mg, 0.234 mmol) was added via microsyringe to each vial and sealed at 23 °C. Aliquots (15  $\mu$ L) were taken at the designated time points, diluted with Et<sub>2</sub>O (1 mL) and analyzed by GC. This procedure was repeated twice more at 2.5, and 1 mol% **1** adjusting the amounts of substrate and PhMe used so that the concentration of substrate is 0.2M. Error bars indicate one standard deviation from the mean.

Experiment with 1 mol% **1**: the data fit to an exponential decay to the equation  $y = 0.21e^{-0.000057x}$ ,  $R^2 = 0.9966$  (left graph). Plotting the  $\ln[N,N\text{-diallyl-}i\text{-tert-butylamine}]$  versus time, the data fit to a linear decay to the equation  $y = -0.00006x - 1.56$ ,  $R^2 = 0.9966$  (right graph).



Experiment with 2.5 mol% **1**: the data fit to an exponential decay to the equation  $y = 0.22e^{-0.00030x}$ ,  $R^2 = 0.9934$  (left graph). Plotting the  $\ln[N,N\text{-diallyl-}tert\text{-butylamine}]$  versus time, the data fit to a linear decay to the equation  $y = -0.00030x - 1.50$ ,  $R^2 = 0.9934$  (right graph).

Experiment with 5 mol% **1**: the data fit to an exponential decay to the equation  $y = 0.24e^{-0.0010x}$ ,  $R^2 = 0.9872$  (left graph). Plotting the  $\ln[N,N\text{-diallyl-}tert\text{-butylamine}]$  versus time, the data fit to a linear decay to the equation  $y = -0.0010x - 1.44$ ,  $R^2 = 0.9934$  (right graph).

The observed rates obtained from these experiments were plotted against the concentration of **1**, and fitted to a line described by the equation  $y = 0.12x - 0.00023$ ,  $R^2 = 0.9821$ .

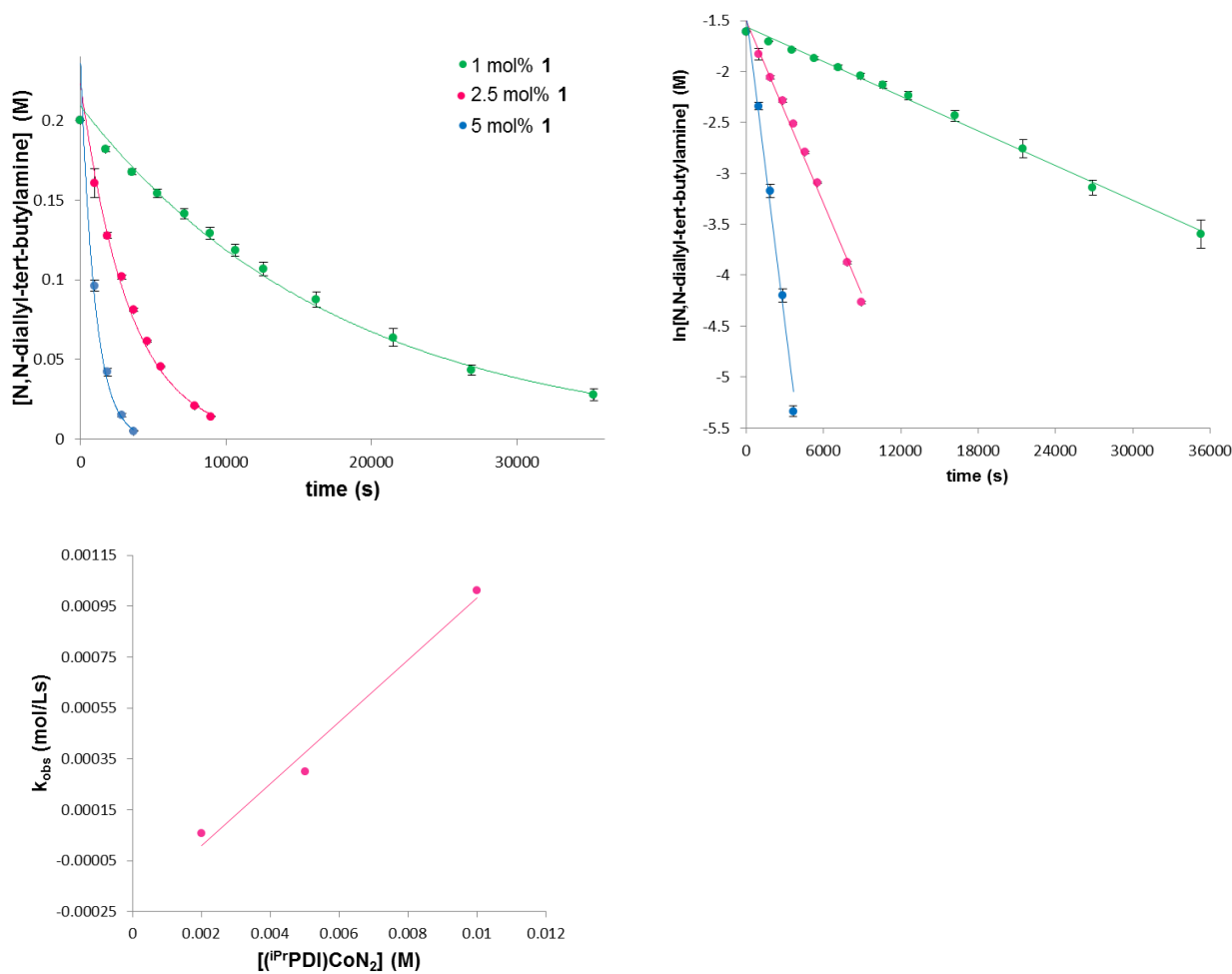


**Figure S21.** Kinetic plots for the cycloaddition of  $N,N$ -diallyl- $tert$ -butylamine in the presence of **1**. Procedure for kinetic experiments reaction of  $(^MePDI)CoN_2$  (**4**) with  $N,N$ -diallyl- $tert$ -butylamine (Figure S21): A stock solution of **4** (15 mg, 0.033 mmol) in PhMe (2.85 g) was prepared and evenly distributed by mass into 3 separate vials.  $N,N$ -diallyl- $tert$ -butylamine (34 mg, 0.209 mmol)

was added via microsyringe to each vial and sealed at 23 °C. Aliquots (15  $\mu$ L) were taken at the designated time points, diluted with Et<sub>2</sub>O (1 mL) and analyzed by GC. This procedure was repeated twice more at 2.5, and 1.25 mol% **4** adjusting the amounts of substrate and PhMe used so that the concentration of substrate is 0.2M. Error bars indicate one standard deviation from the mean.

Experiment with 1.25 mol% **4**: the data fit to a linear decay to the equation  $y = -0.000060x + 0.19$ ,  $R^2 = 0.9930$  (left graph).

Experiment with 2.5 mol% **4**: the data fit to a linear decay to the equation  $y = -0.00013x + 0.19$ ,  $R^2 = 0.9967$  (left graph).

Experiment with 5 mol% **4**: the data fit to a linear decay to the equation  $y = -0.00033x + 0.19$ ,  $R^2 = 0.9942$  (left graph).

The observed rates obtained from these experiments were plotted against the concentration of **4**, and fitted to a line described by the equation  $y = 0.036x - 0.00004$ ,  $R^2 = 0.9916$ .

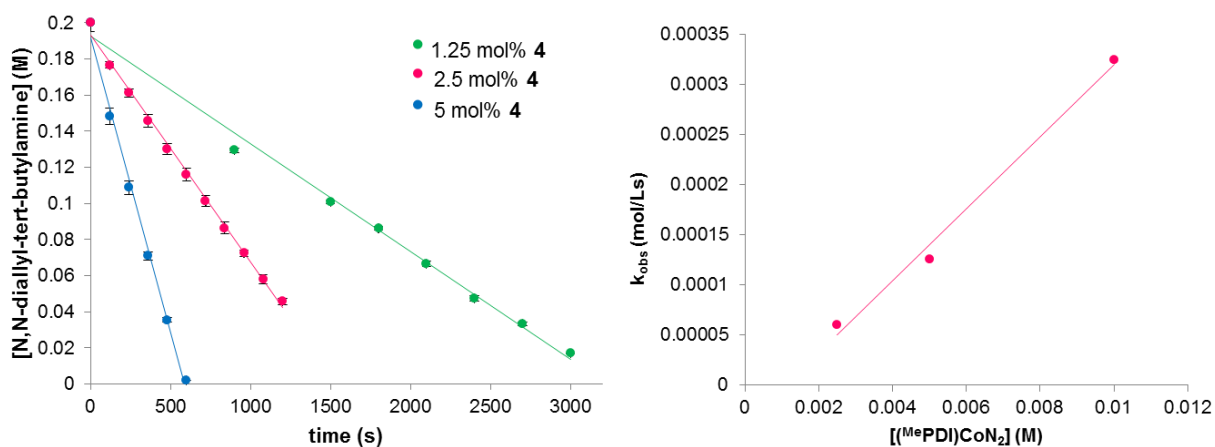


**Figure S22.** Kinetic plots for the cycloaddition of *N,N*-diallyl-*tert*-butylamine in the presence of **4**.

## VI. Additional Computational Results.

### a. DFT Input File examples

#### Geometry optimization

```
! UKS B3LYP RIJCOSX SlowConv TightSCF def2-SV(P) def2-SVP/J Normalprint UCO OPT  
PAL8
```

```
%basis NewGTO 27 "def2-TZVP(-f)" end  
    NewGTO 7 "def2-TZVP(-f)" end  
    NewAuxGTO 27 "def2-TZVP/J" end  
    NewAuxGTO 7 "def2-TZVP/J" end  
end
```

```
%scf brokenSym 2,1
```

```
    MaxIter 500
```

```
    TolE 1e-7
```

```
    TolErr 1e-6
```

```
end
```

```
*xyz 0 2
```

```
xyz coordinates from X-ray structure
```

```
*
```

#### EPR parameter calculations

```
! UKS B3LYP TightSCF SlowConv def2-SVP Grid4 NoFinalGrid PAL8
```

```
%basis NewGTO 27 "CP(PPP)" end
```

```
    NewGTO 7 "IGLO-III" end
```

```
    NewGTO 1 "IGLO-III" end
```

```
end
```

```
%method SpecialGridAtoms 27, 7, 1
```

```
    SpecialGridAcc 11, 9, 9
```

```
end
```

```
%scf MaxIter 500
```

```
    TolE 1e-7
```

```
    TolErr 1e-6
```

```

end
*xyz 0 2
xyz coordinates from geometry optimization
*
%eprnmr gtensor 1
ori -3
Nuclei = all Co { aiso }
Nuclei = all N { aiso }
Nuclei = all H { aiso }
end

```

### **b. Coordinates from Geometry Optimization**

iPrtbPDICo-diene compound 8

Co	-0.075375	-0.001881	0.007057
N	-0.011705	1.963488	0.043014
O	-4.191704	-8.312801	0.578944
N	-2.557616	0.858201	0.093769
N	-1.131662	-3.603578	0.131032
N	2.210512	0.385280	-0.062961
C	3.718642	-1.081128	-1.347168
C	-1.129071	2.776928	0.134041
C	-5.579846	-0.976645	-1.081708
H	-6.052345	-1.268811	-2.024210
C	-3.517550	4.428493	-0.185406
H	-3.525495	4.327958	-1.287345
H	-4.383019	5.059415	0.087213
C	1.401625	3.954176	0.081146
C	-1.018113	4.176797	0.161205
C	1.243630	2.553659	0.040071

C	-4.426813	-0.179739	-1.108958
C	-2.455135	2.143989	0.206970
C	0.261021	4.755608	0.112533
H	0.362216	5.845907	0.113910
C	3.295481	-0.544822	-0.096186
C	-2.219601	5.090141	0.267919
H	-2.324350	5.412807	1.324544
H	-2.024510	6.013568	-0.306308
C	-3.896102	0.334696	-2.447418
H	-2.865403	0.678464	-2.274566
C	4.821349	-2.066454	1.035190
H	5.274134	-2.440502	1.958711
C	-4.424348	-0.186632	1.356798
C	-6.145933	-1.403473	0.119694
H	-7.039755	-2.034920	0.118314
C	-5.573887	-0.991261	1.321100
H	-6.039133	-1.294673	2.264060
C	-3.413263	-7.193656	0.514034
C	3.901679	-1.008307	1.106234
C	-3.817353	0.191169	0.125649
C	-3.922496	0.306546	2.715324
H	-3.005810	0.891166	2.540436
C	-4.688866	1.564120	-2.937103
H	-5.747914	1.306533	-3.126331
H	-4.260745	1.952976	-3.880133
H	-4.665689	2.380518	-2.195723
C	-4.949079	1.247101	3.381437
H	-5.294743	2.037424	2.694542
H	-4.509844	1.733263	4.273228

H	-5.842662	0.687189	3.713067
C	3.256923	-0.490274	-2.678920
H	2.423845	0.192386	-2.459445
C	-2.383611	-6.884067	1.418828
H	-2.132478	-7.561170	2.238782
C	3.654438	-0.359455	2.469561
H	2.898526	0.429651	2.333814
C	-1.908538	-4.793737	0.227331
C	-2.940480	-5.122641	-0.675880
H	-3.204330	-4.441470	-1.487472
C	-3.650801	3.051922	0.463845
H	-3.746533	3.188018	1.559320
H	-4.571917	2.544837	0.139396
C	3.850618	3.714443	-0.497596
H	3.713154	3.670278	-1.594759
H	4.849242	4.150712	-0.311692
C	4.652211	-2.126674	-1.358681
H	4.974825	-2.544274	-2.317565
C	2.405275	1.676560	0.002034
C	-3.672196	-6.304267	-0.538821
H	-4.474592	-6.548472	-1.240842
C	3.110488	-1.345369	3.519273
H	3.864722	-2.108342	3.783067
H	2.212629	-1.871562	3.156663
H	2.840712	-0.810659	4.448884
C	-4.130719	-9.119006	1.729584
H	-3.143552	-9.610052	1.847968
H	-4.897946	-9.900337	1.605471
H	-4.350724	-8.537474	2.648111

C	-1.639528	-5.711196	1.260386
H	-0.819091	-5.508040	1.954466
C	5.187625	-2.642671	-0.179401
H	5.900924	-3.472705	-0.208858
C	-3.851345	-0.739823	-3.548762
H	-3.316511	-1.645369	-3.212985
H	-3.326909	-0.350109	-4.439951
H	-4.860829	-1.048978	-3.876103
C	2.769561	4.595032	0.125143
H	2.729574	5.582715	-0.367357
H	3.031599	4.794149	1.184704
C	3.784017	2.305752	0.092336
H	4.072313	2.359349	1.160373
H	4.524090	1.642556	-0.382265
C	-3.564151	-0.831362	3.690740
H	-4.458903	-1.408054	3.989322
H	-3.113654	-0.417323	4.611647
H	-2.843178	-1.537841	3.250801
C	4.368672	0.358133	-3.328292
H	5.224681	-0.271004	-3.634764
H	4.753821	1.129630	-2.638995
H	3.985334	0.870468	-4.231246
C	4.936410	0.317835	3.006024
H	5.694821	-0.433493	3.291182
H	4.710360	0.921590	3.905241
H	5.398693	0.981456	2.254924
C	2.748687	-1.545517	-3.678714
H	3.568566	-2.189274	-4.045719
H	2.297555	-1.054332	-4.560594

H	1.982570	-2.197448	-3.228206
C	-0.298081	-0.682953	-1.981159
C	-0.111661	-1.854895	-1.292390
C	-0.074604	-1.757683	1.406422
C	-1.215142	-2.862672	-1.120944
H	-2.194450	-2.351443	-1.235424
H	-1.123014	-3.596242	-1.942093
C	-0.175620	-0.540166	2.033883
C	-1.229976	-2.708410	1.288238
H	-1.259074	-3.333789	2.194969
H	-2.182104	-2.141234	1.256936
H	0.701294	-0.057357	2.451018
H	-1.286027	-0.407676	-2.331092
H	0.909790	-2.211483	1.292973
H	0.527801	-0.176087	-2.464551
H	-1.129415	-0.181574	2.405957
H	0.897014	-2.248951	-1.173553



## VII. References

- <sup>1</sup> Salvi, L.; Davis, N. R.; Ali, S. Z.; Buchwald, S. L. *Org. Lett.* **2012**, *14*, 170.
- <sup>2</sup> Bowman, A. C.; Milsman, C.; Atienza, C. C. H.; Lobkovsky, E.; Wieghardt, K.; Chirik, P. J. *J. Am. Chem. Soc.* **2010**, *132*, 1676.
- <sup>3</sup> Neese, F., Orca: an ab initio, DFT and Semiempirical Electronic Structure Package, Version 2.8, Revision 2287; Institut für Physikalische und Theoretische Chemie, Universität Bonn: Bonn, Germany, 2010.
- <sup>4</sup> Perdew, J. P. *Phys. Rev. B* **1986**, *33*, 8822.
- <sup>5</sup> Perdew, J. P. *Phys. Rev. B* **1986**, *34*, 7406.
- <sup>6</sup> Lee, C. T.; Yang, W. T.; Parr, R. G.; *Phys. Rev. B* **1988**, *37*, 785.
- <sup>7</sup> F. Neese, E. I. Solomon In *Magnetism: From Molecules to Materials*; J. S. Miller, M. Drillon, Eds.; Wiley: New York, 2002; Vol. 4, p 345.
- <sup>8</sup> Schäfer, A.; Horn, H.; Ahlrichs, R. *J. Chem. Phys.* **1992**, *97*, 2571.
- <sup>9</sup> Schäfer, A.; Huber, C.; Ahlrichs, R. *J. Chem. Phys.* **1994**, *100*, 5829.
- <sup>10</sup> Weigend, F.; Ahlrichs, R. *Phys. Chem. Chem. Phys.* **2005**, *7*, 3297.
- <sup>11</sup> Eichkorn, K.; Weigend, F.; Treutler, O.; Ahlrichs, R. *Theor. Chem. Acc.* **1997**, *97*, 119.
- <sup>12</sup> Eichkorn, K.; Treutler, O.; Öhm, H.; Häser, M.; Ahlrichs, R. *Chem. Phys. Lett.* **1995**, *240*, 283.
- <sup>13</sup> Eichkorn, K.; Treutler, O.; Öhm, H.; Häser, M.; Ahlrichs, R. *Chem. Phys. Lett.* **1995**, *242*, 652.
- <sup>14</sup> Neese, F.; Wennmohs, F.; Hansen, A.; Becker, U. *Chem. Phys.* **2009**, *356*, 98.
- <sup>15</sup> Kossmann, S.; Neese, F. *Chem. Phys. Lett.* **2009**, *481*, 240.
- <sup>16</sup> Neese, F. *J. Comput. Chem.* **2003**, *24*, 1740.
- <sup>17</sup> Ginsberg, A. P. *J. Am. Chem. Soc.* **1980**, *102*, 111.
- <sup>18</sup> Noodleman, L.; Peng, C. Y.; Case, D. A.; Mouesca, J. M. *Coord. Chem. Rev.* **1995**, *144*, 199.
- <sup>19</sup> Kirchner, B.; Wennmohs, F.; Ye, S.; Neese, F. *Curr. Opin. Chem. Biol.* **2007**, *11*, 134.
- <sup>20</sup> Neese, F. *J. Phys. Chem. Solids* **2004**, *65*, 781.
- <sup>21</sup> Pettersen, E. F.; Goddard, T. D.; Huang, C. C.; Couch, G. S.; Greenblatt, D. M.; Meng, E. C.; Ferrin, T. E. *J. Comput. Chem.* **2004**, *25*, 1605.
- <sup>22</sup> McTavish, S.; Britovsek, G. J. P.; Smit, T. M.; Gibson, V. C.; White, A. J. P.; Williams, D. J. *J. Mol. Catal. A: Chemical* **2007**, *261*, 293.

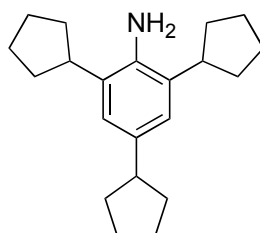
- <sup>23</sup> Obligacion, J. V.; Chirik, P. J. *J. Am. Chem. Soc.* **2013**, *135*, 19107.
- <sup>24</sup> Salvi, L.; Davis, N. R.; Ali, S. Z.; Buchwald, S. L. *Org. Lett.* **2012**, *14*, 170.
- <sup>25</sup> Behloul, C.; Guijarro, D.; Yus, M. *Synthesis* **2004**, 1274.
- <sup>26</sup> Ramachary, D. B.; Narayana, V. V. *Eur. J. Org. Chem.* **2011**, 3514.
- <sup>27</sup> Bouwkamp, M. W.; Bowman, A. C.; Lobkovsky, E.; Chirik, P. J. *J. Am. Chem. Soc.* **2006**, 13340.
- <sup>28</sup> Daeffler, C. S.; Grubbs, R. H. *Org. Lett.* **2011**, *13*, 6429.
- <sup>29</sup> Carda, M.; Castillo, E.; Rodríguez, S.; Uriel, S.; Marco, J. A. *Synlett* **1999**, 1639.
- <sup>30</sup> Ben Ammar, H.; Le Nôtre, J.; Salem, M.; Kaddachi, M. T.; Toupet, L.; Renaud, J.-L.; Bruneau, C.; Dixneuf, P. H. *Eur. J. Inorg. Chem.* **2003**, 4055.
- <sup>31</sup> Ghosh, S.; Raychaudhuri, S. R.; Salomon, R. G. *J. Org. Chem.* **1987**, *52*, 83.
- <sup>32</sup> Hoyt, J. M.; Sylvester, K. T.; Semproni, S. P.; Chirik, P. J. *J. Am. Chem. Soc.* **2013**, *135*, 4862.

### VIII. <sup>1</sup>H and <sup>13</sup>C NMR Spectra of Organic Compounds

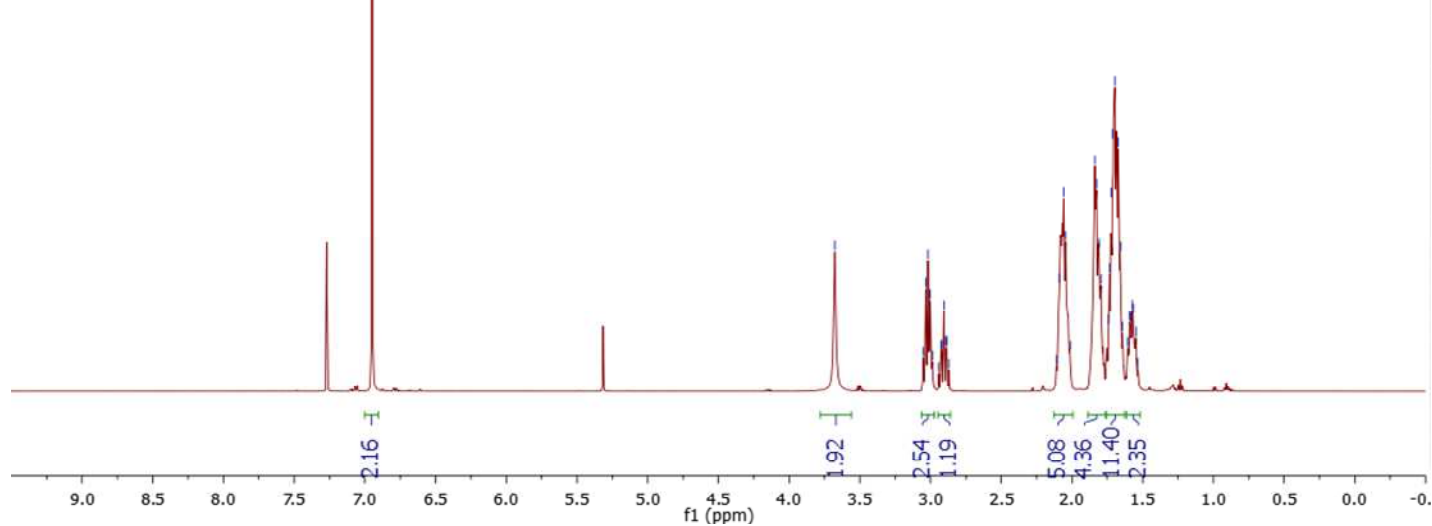
VAS-III-205col\_A3\_84-.10.fid  
2,4,6-tricyclopentylaniline

3.68  
3.05  
3.03  
3.02  
3.00  
2.99  
2.94  
2.93  
2.92  
2.91  
2.89  
2.89  
2.87

2.09  
2.06  
2.04  
1.84  
1.83  
1.81  
1.80  
1.73  
1.72  
1.71  
1.70  
1.67  
1.66  
1.57  
1.57



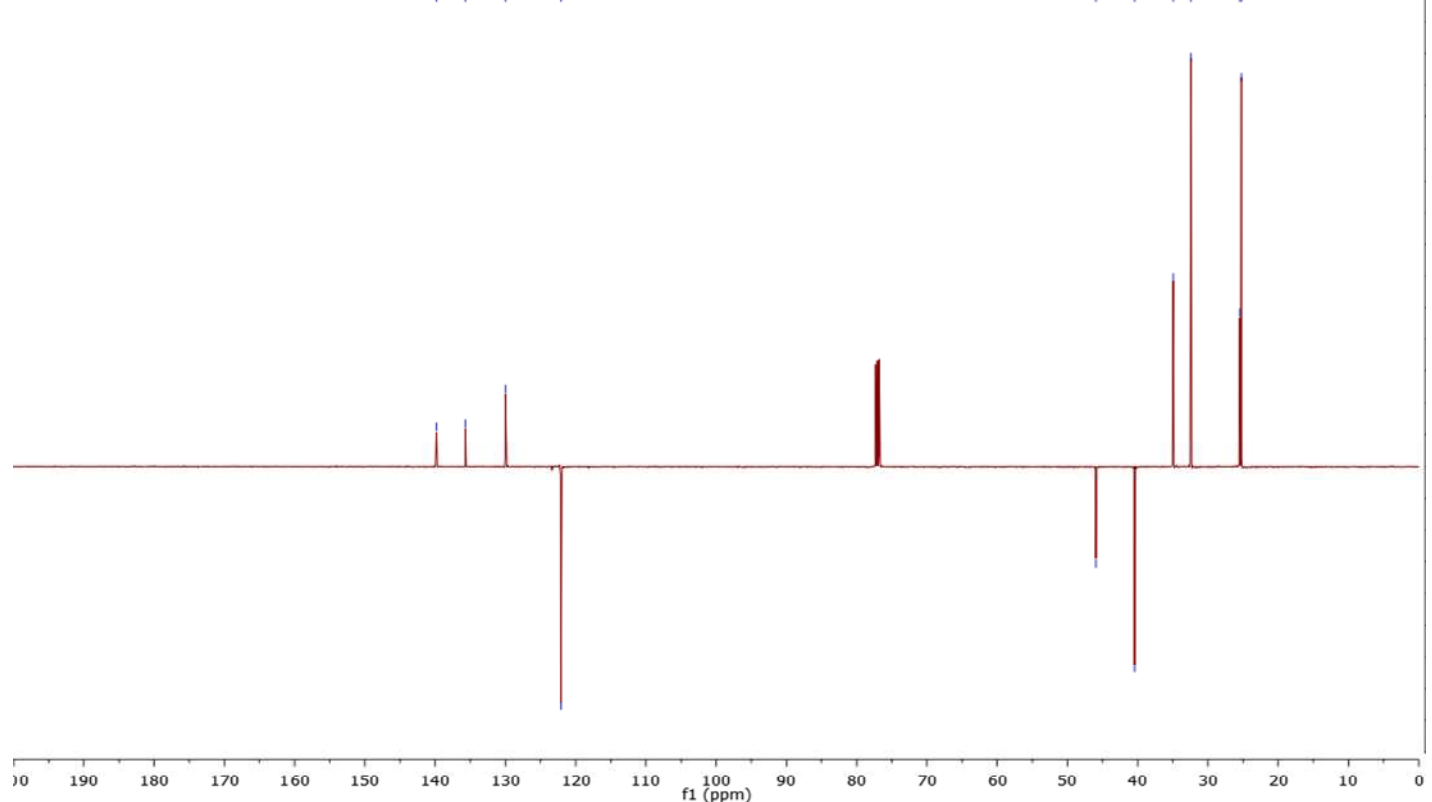
2,4,6-tricyclopentylaniline



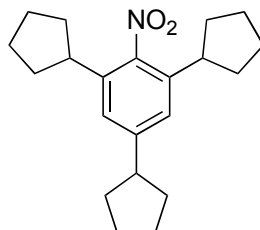
VAS-III-205col\_A3\_84-.11.fid  
2,4,6-tricyclopentylaniline

~139.81  
~135.71  
~130.00  
-122.11

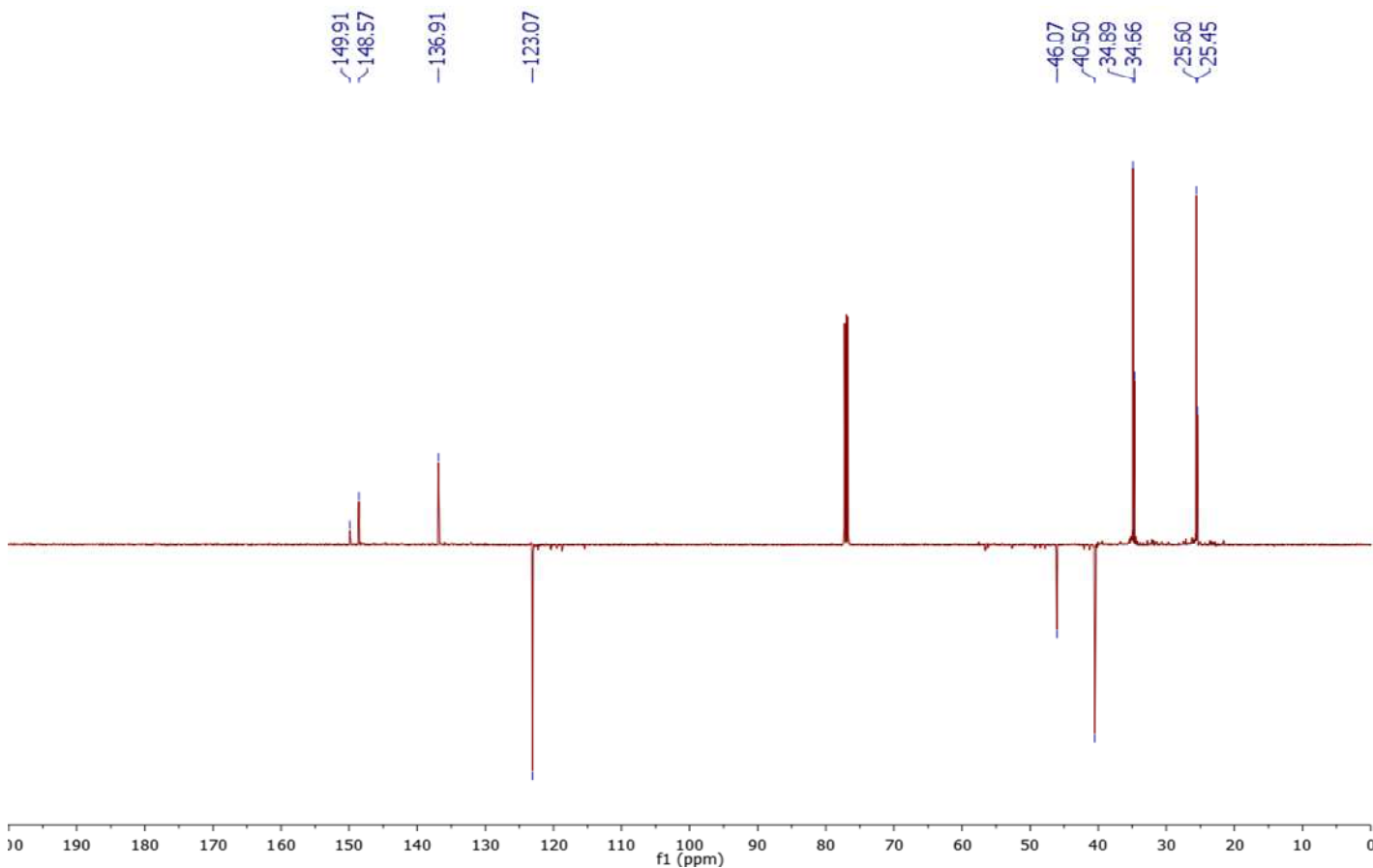
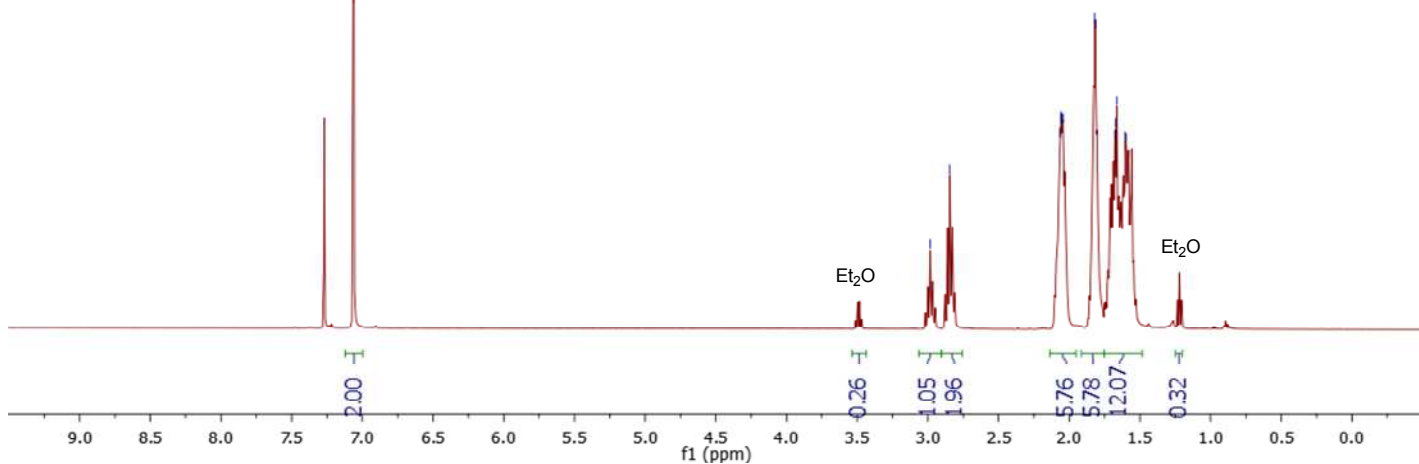
~45.95  
~40.43  
~34.92  
~32.40  
~25.45  
~25.24



2.98  
2.84  
2.06  
2.06  
2.05  
2.04  
1.82  
1.81  
1.68  
1.67  
1.66  
1.60

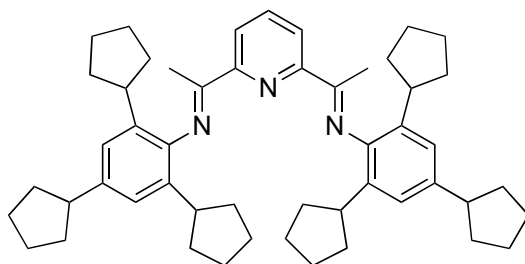


2,4,6-tricyclopentylnitrobenzene

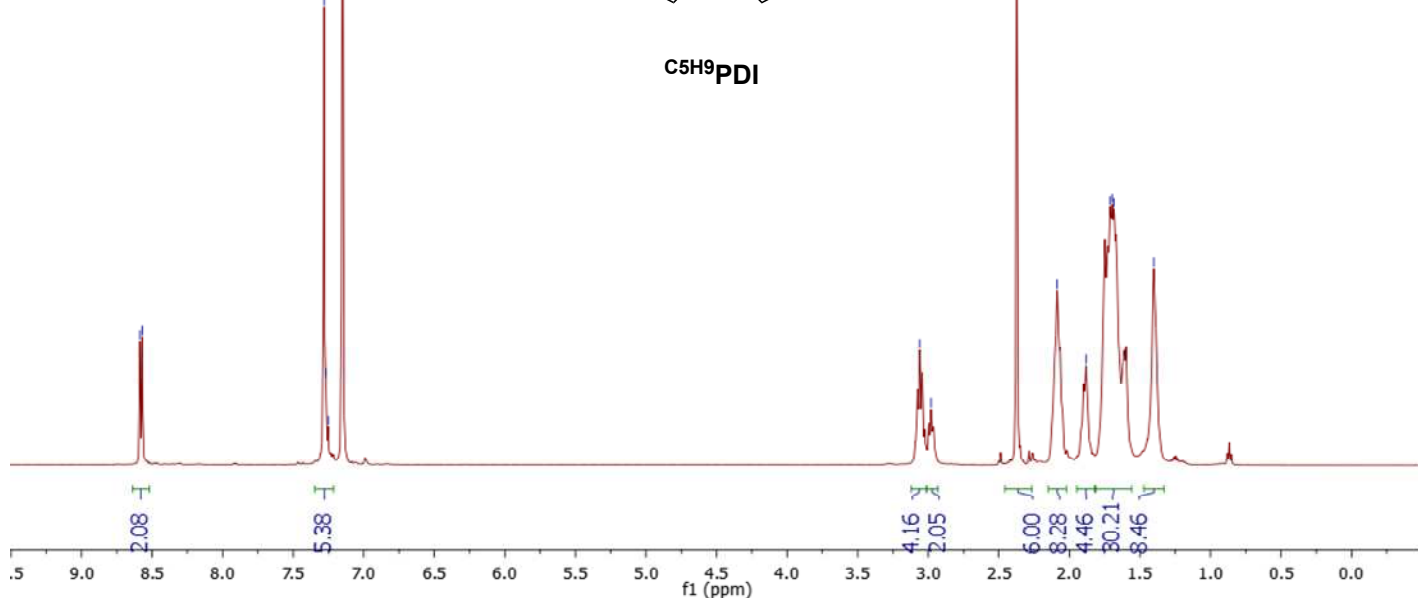


VAS-III-213a\_A2\_92-.10.fid  
C5H9PDI  
PROTON.PU C6D6 /opt/topspin3.0 vschmidt 92

3.06  
2.98  
2.37  
2.09  
1.88  
1.71  
1.70  
1.68  
1.40



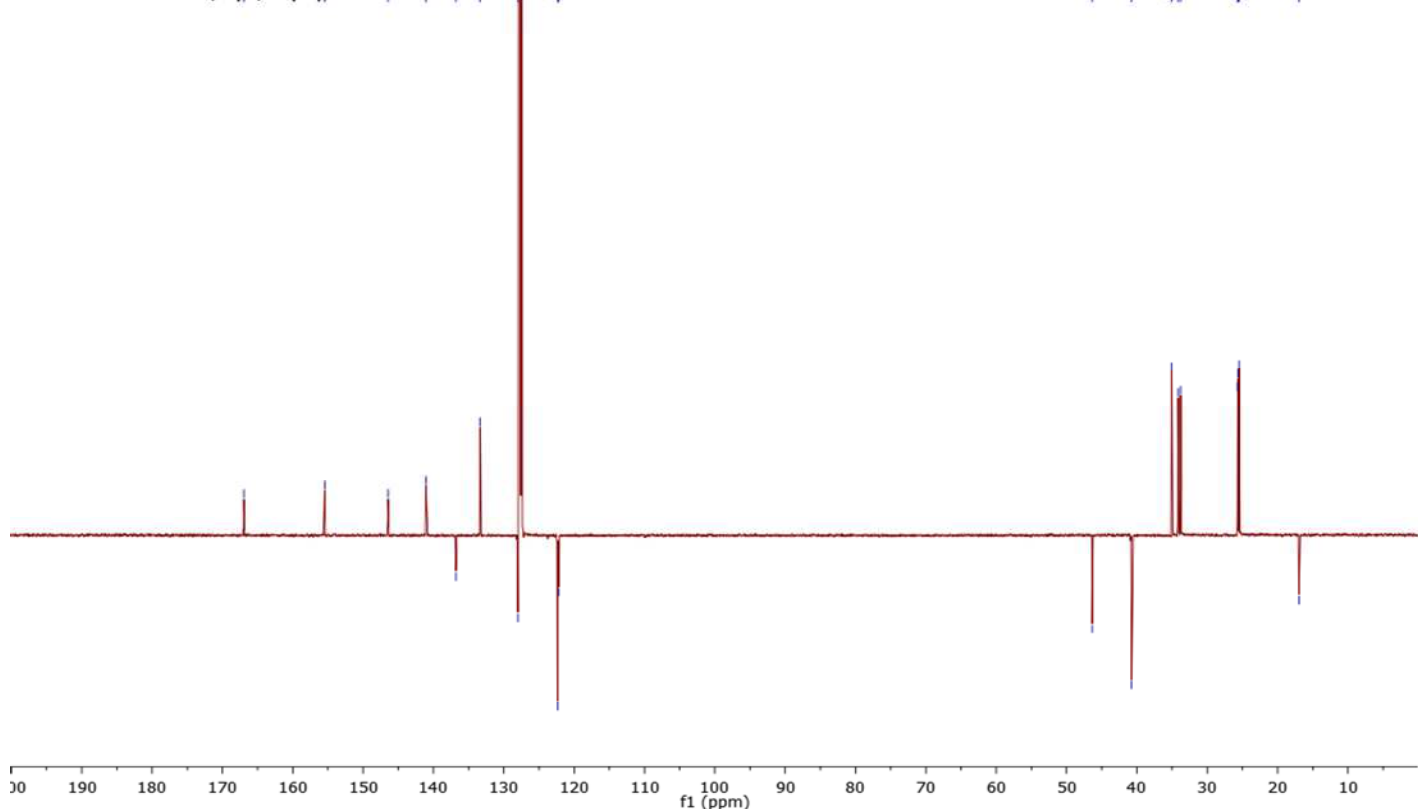
C5H9PDI

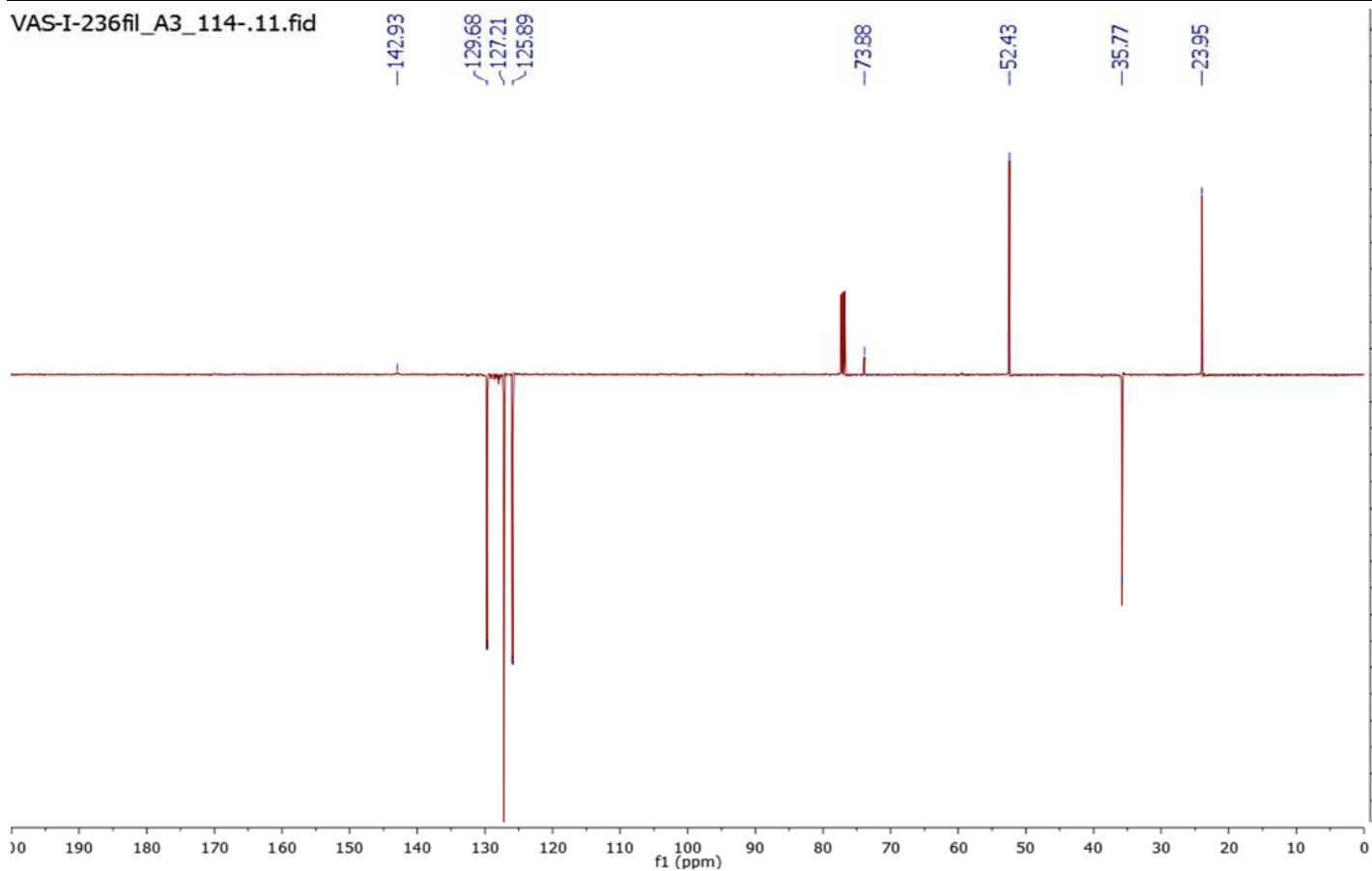
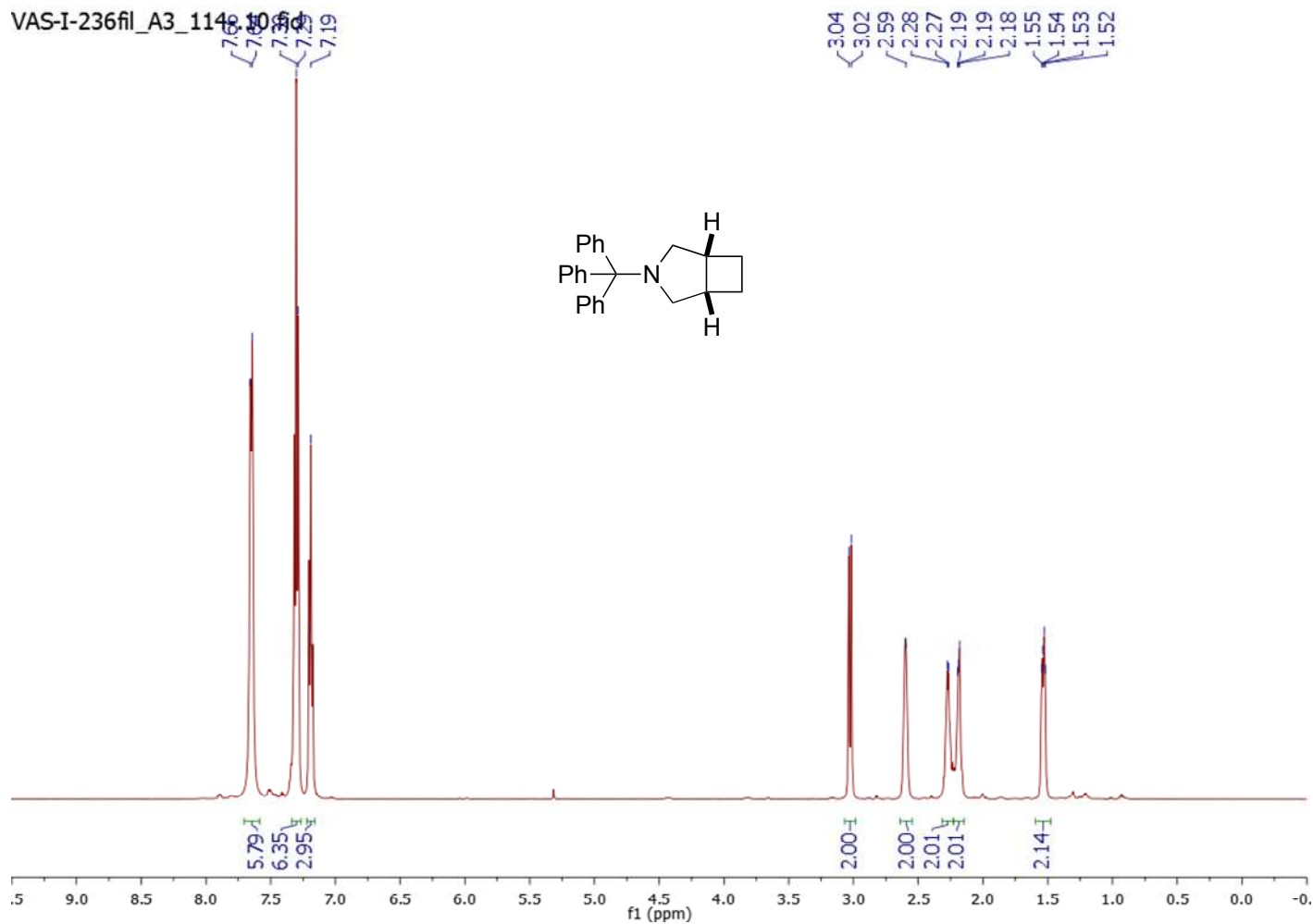


VAS-III-213a\_A2\_92-.11.fid  
C5H9PDI  
C13APT.PU C6D6 /opt/topspin3.0 vschmidt 92

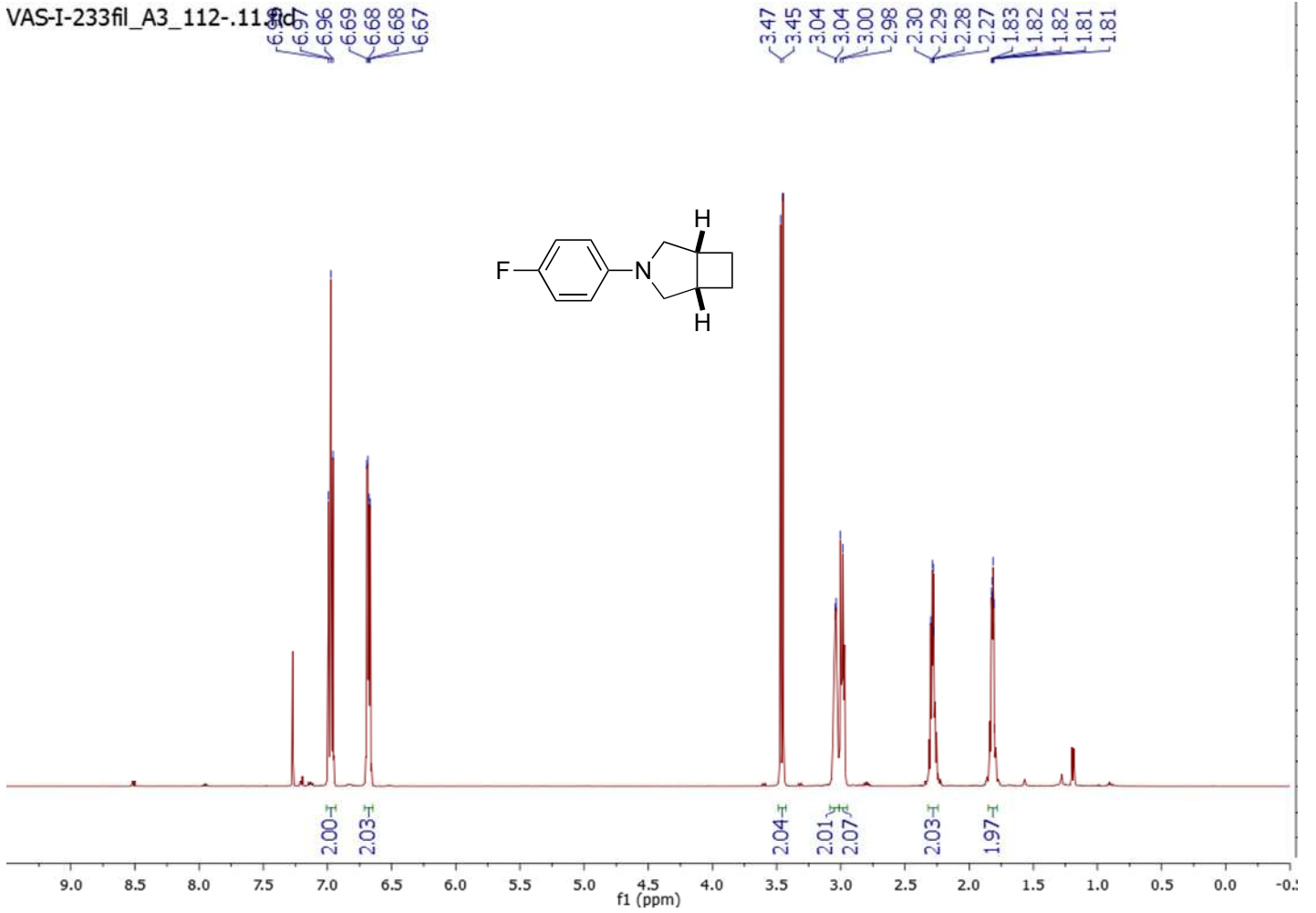
166.87  
155.4  
146.46  
141.08  
136.81  
133.35  
127.97  
122.37  
122.22  
122.22

46.37  
40.75  
35.06  
34.16  
33.78  
25.69  
25.65  
25.48  
-16.97

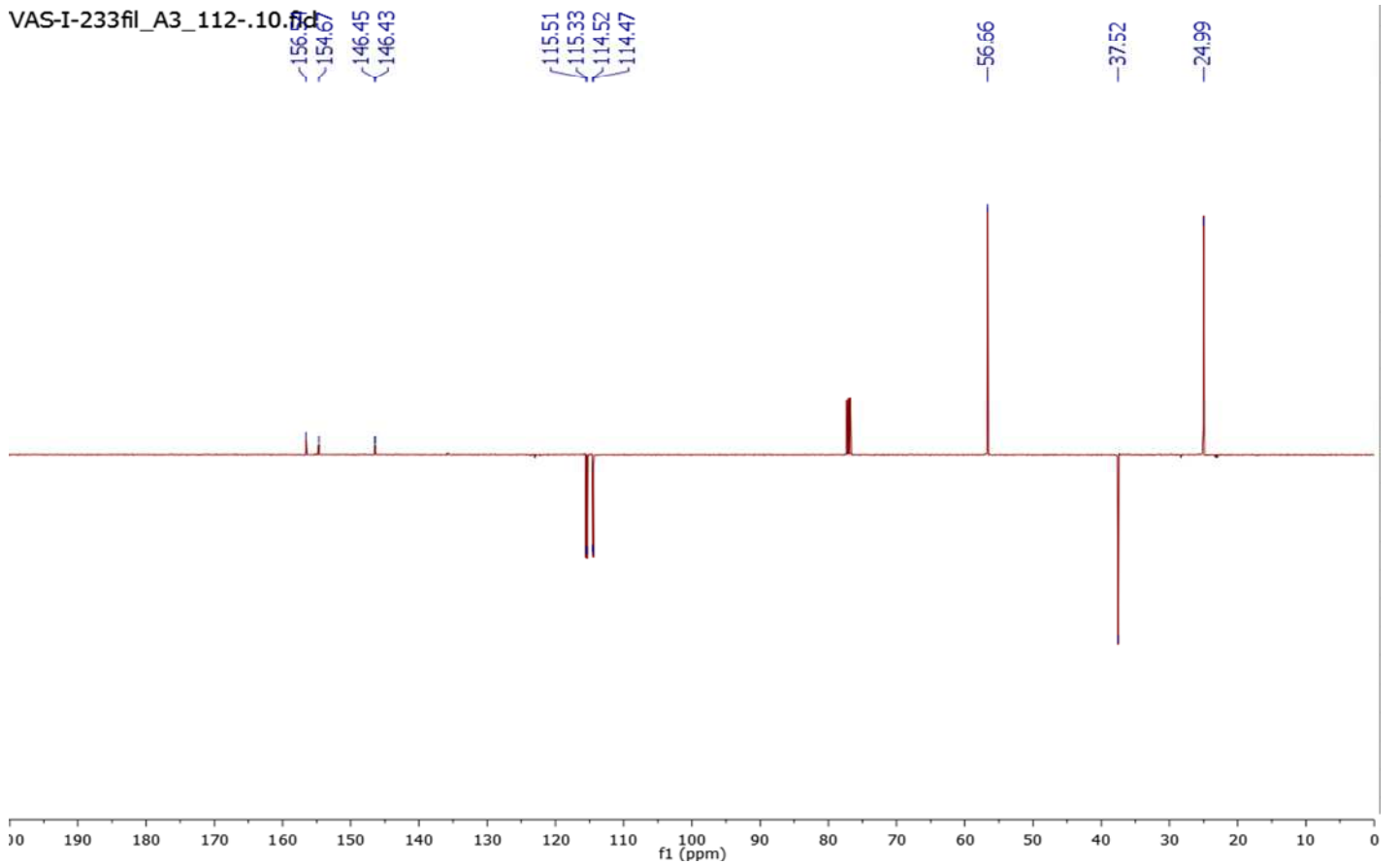




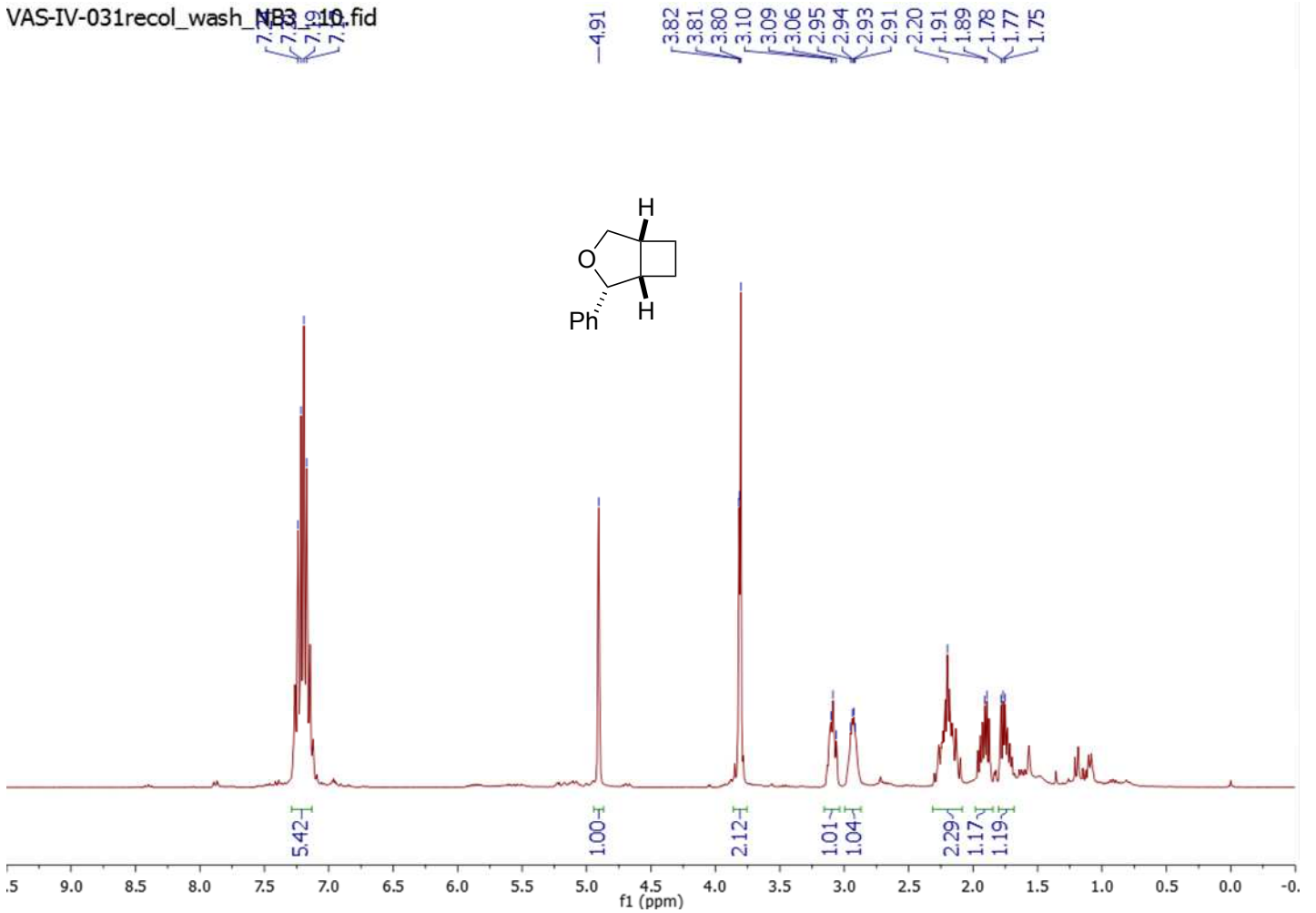
VAS-I-233fil\_A3\_112-.111



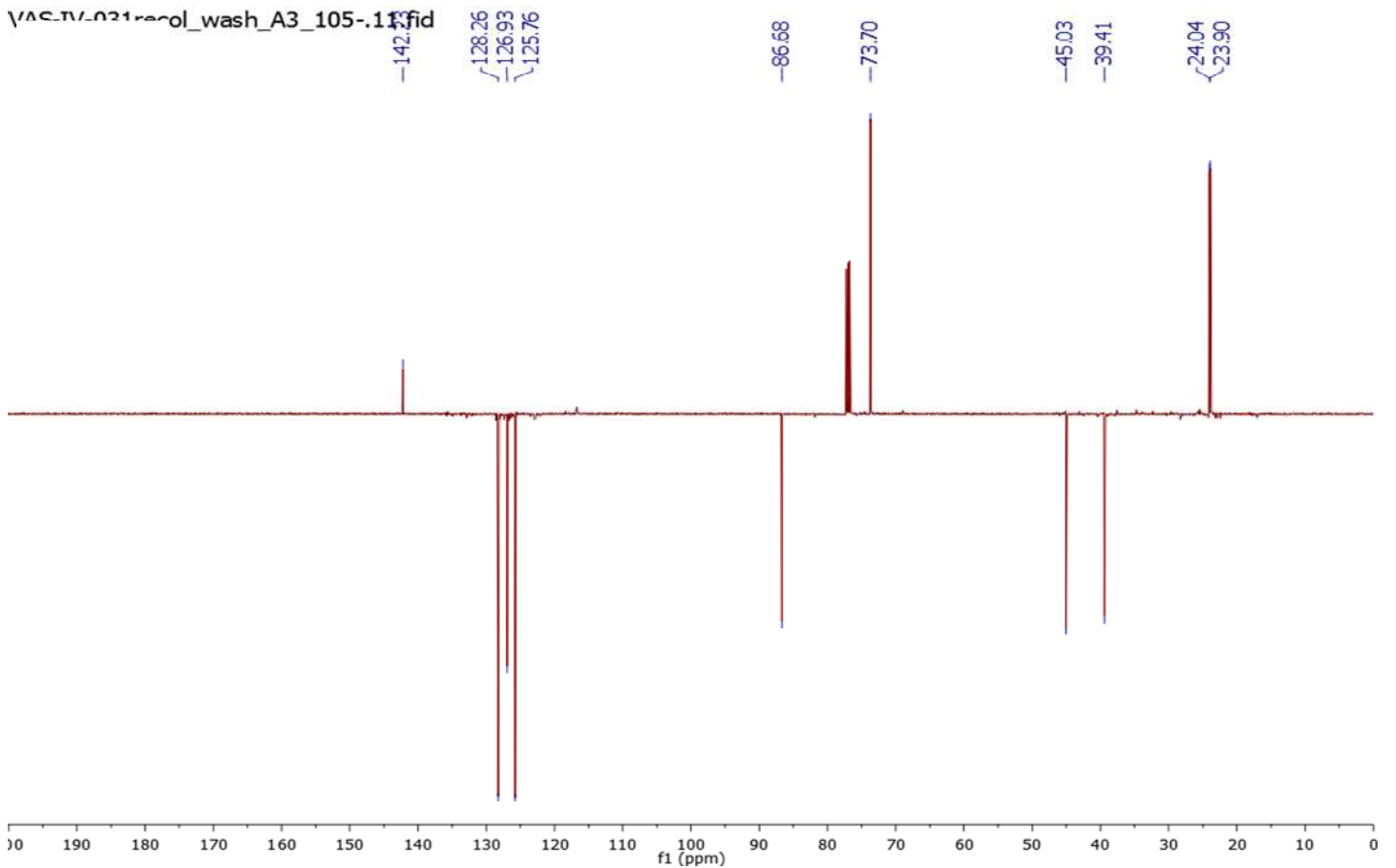
VAS-I-233fil\_A3\_112-.101



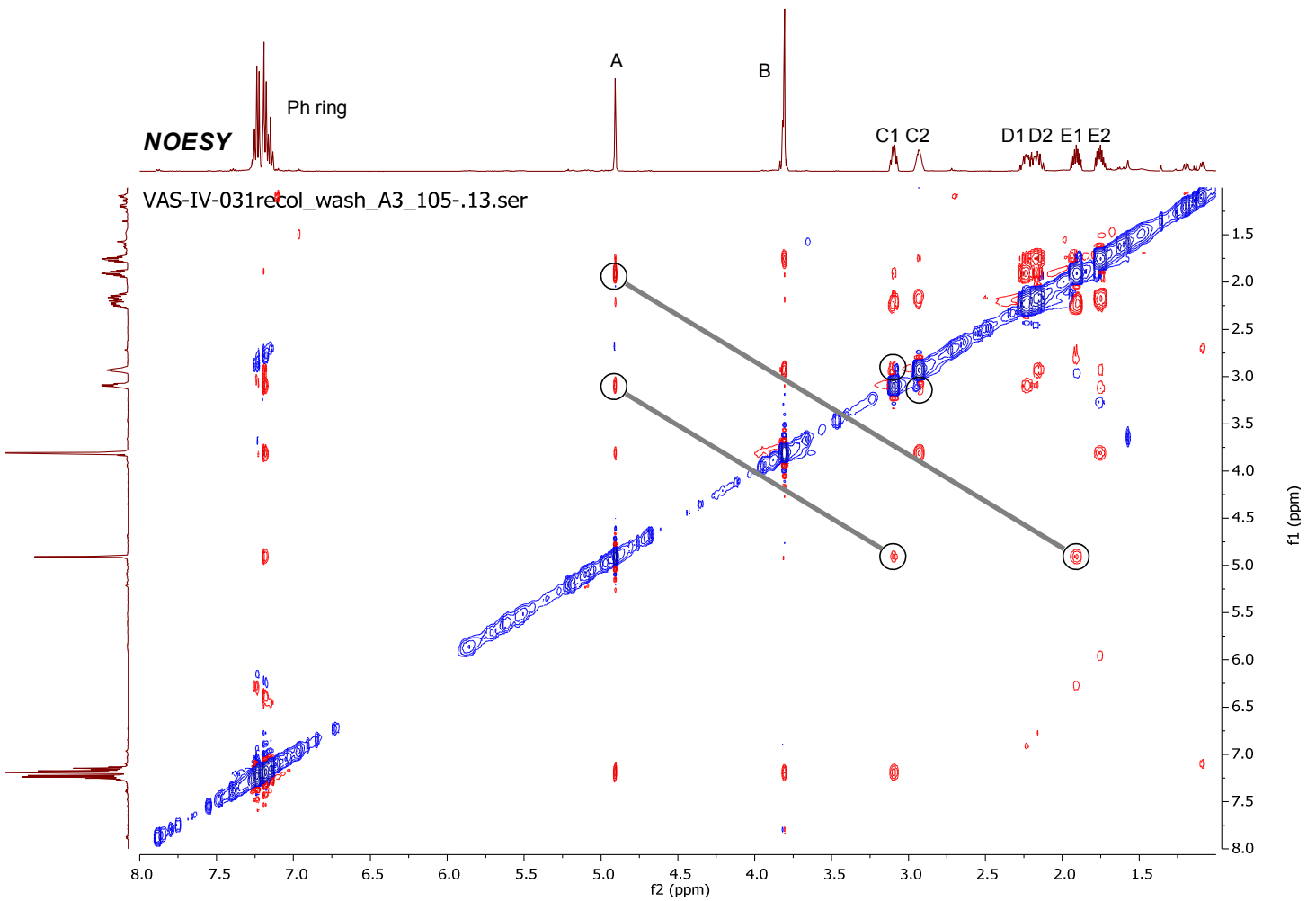
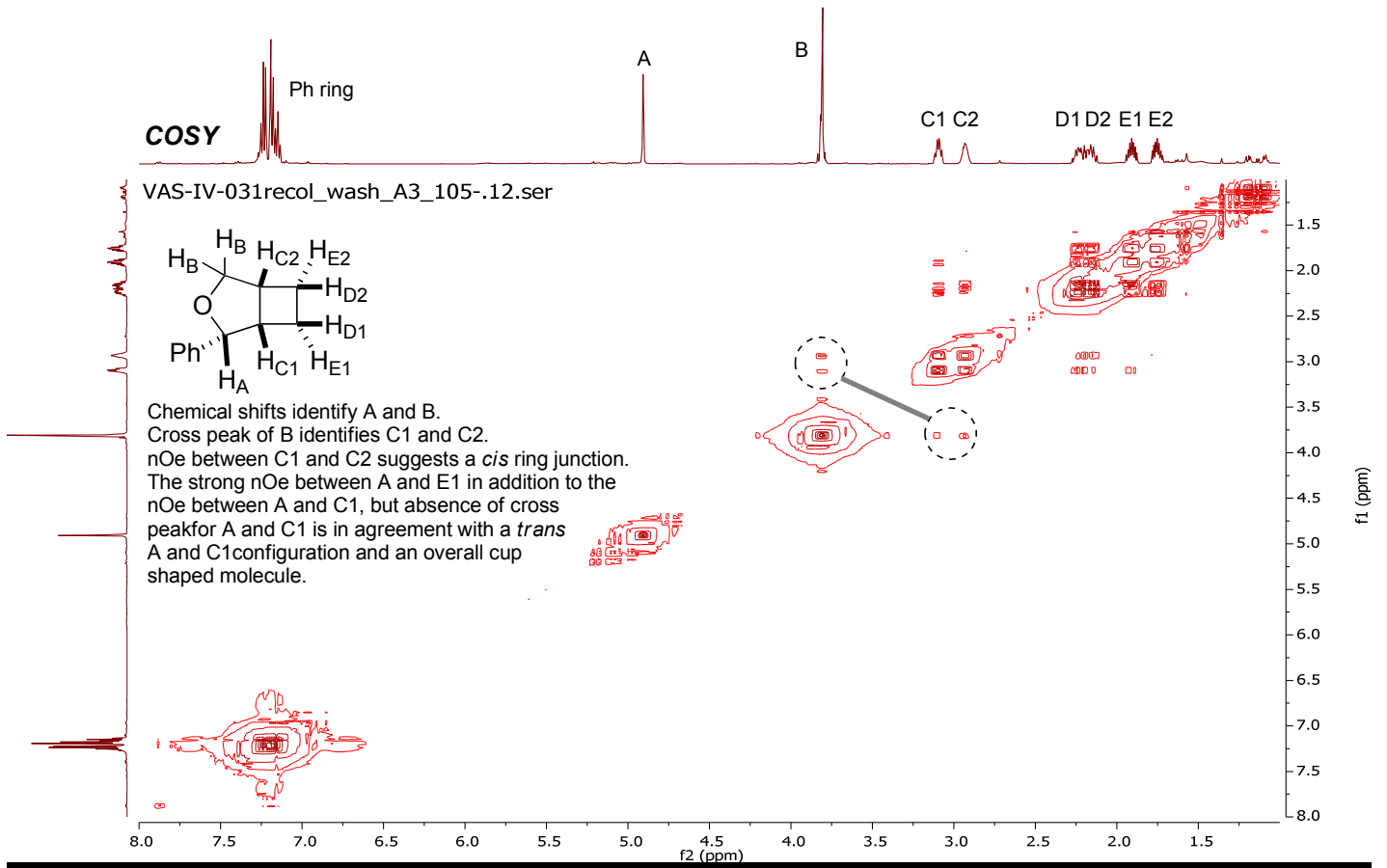
VAS-IV-031recol\_wash\_NB3\_10.fid

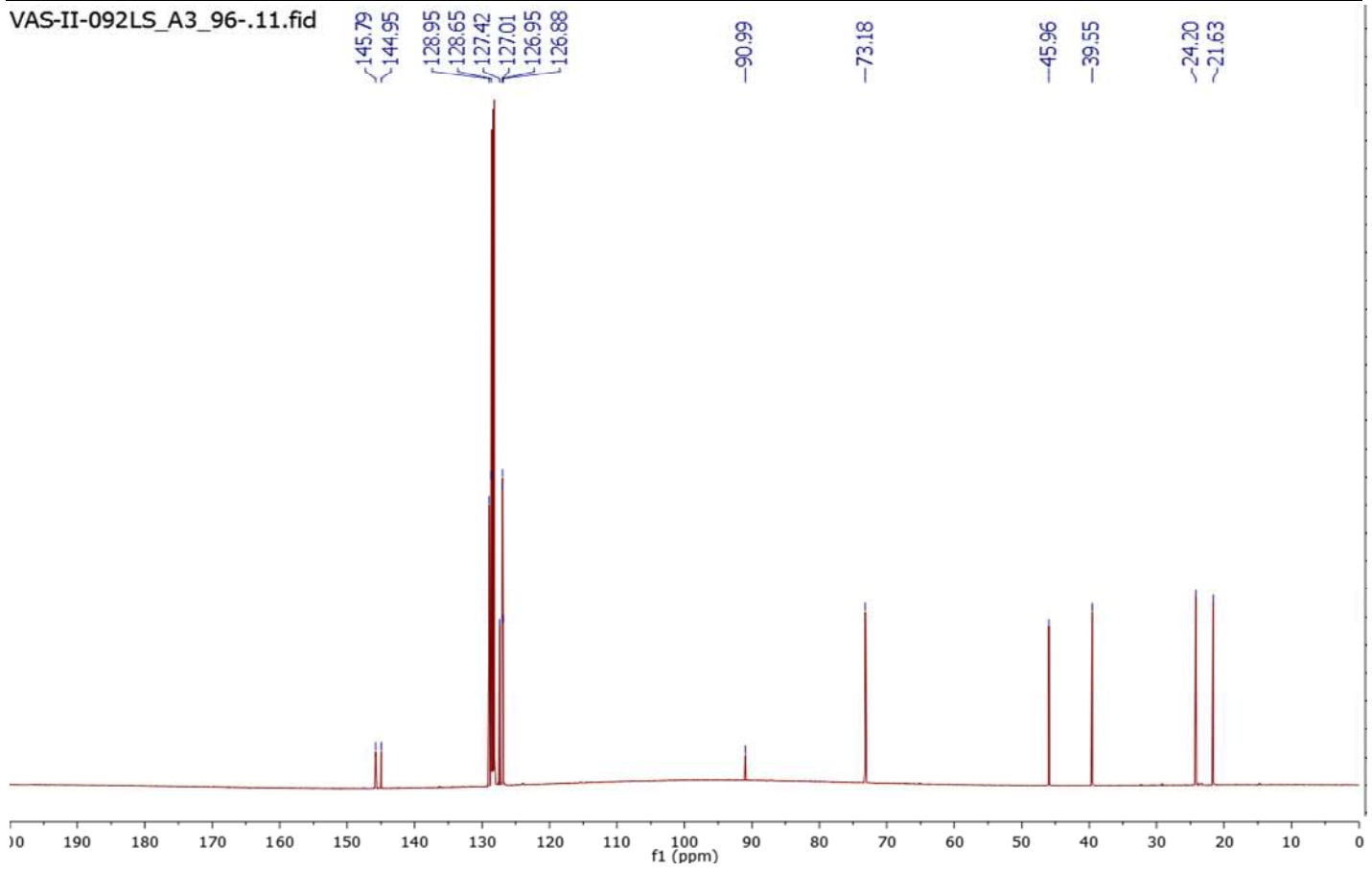
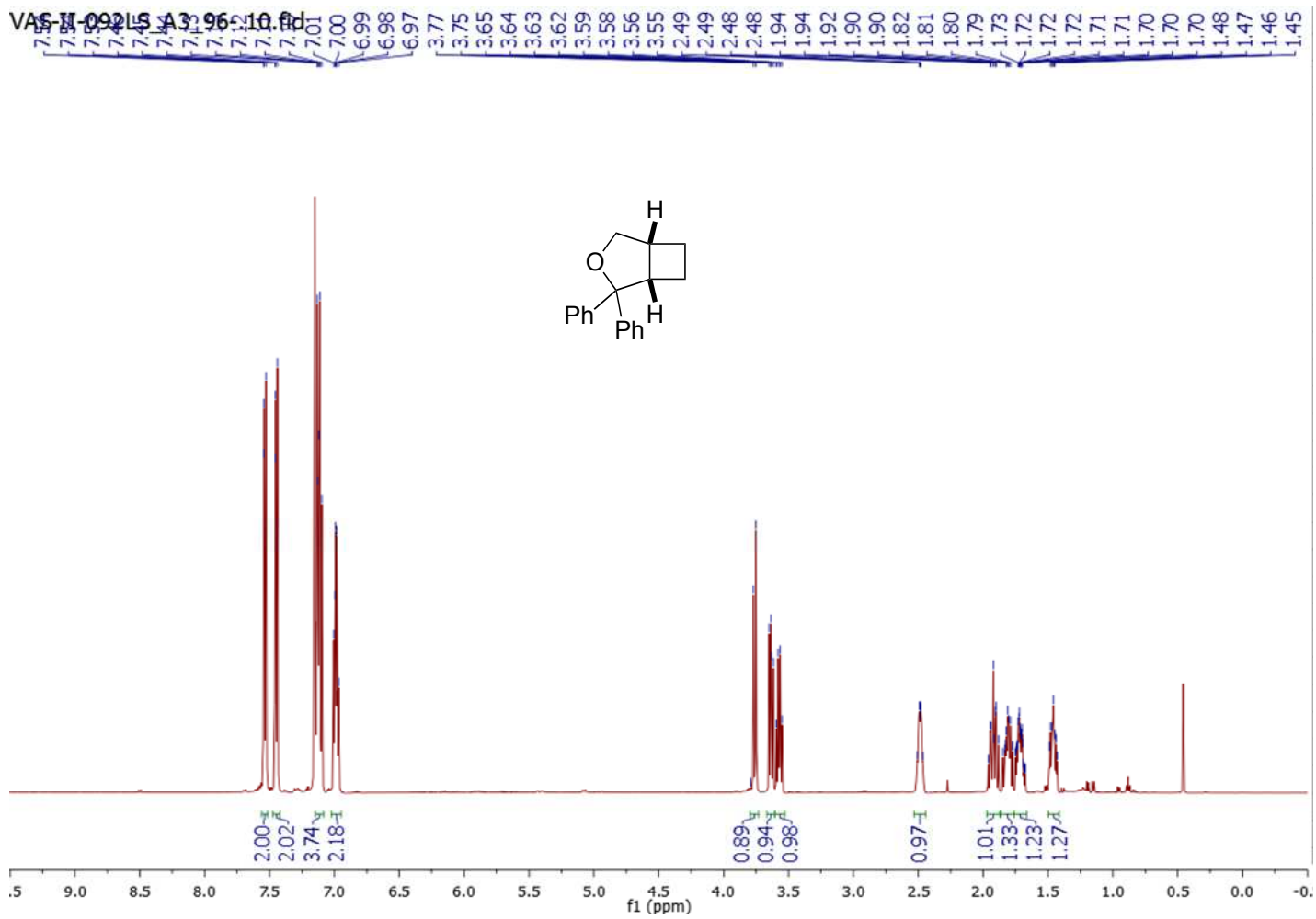


VAS-IV-031recol\_wash\_A3\_105-11.fid





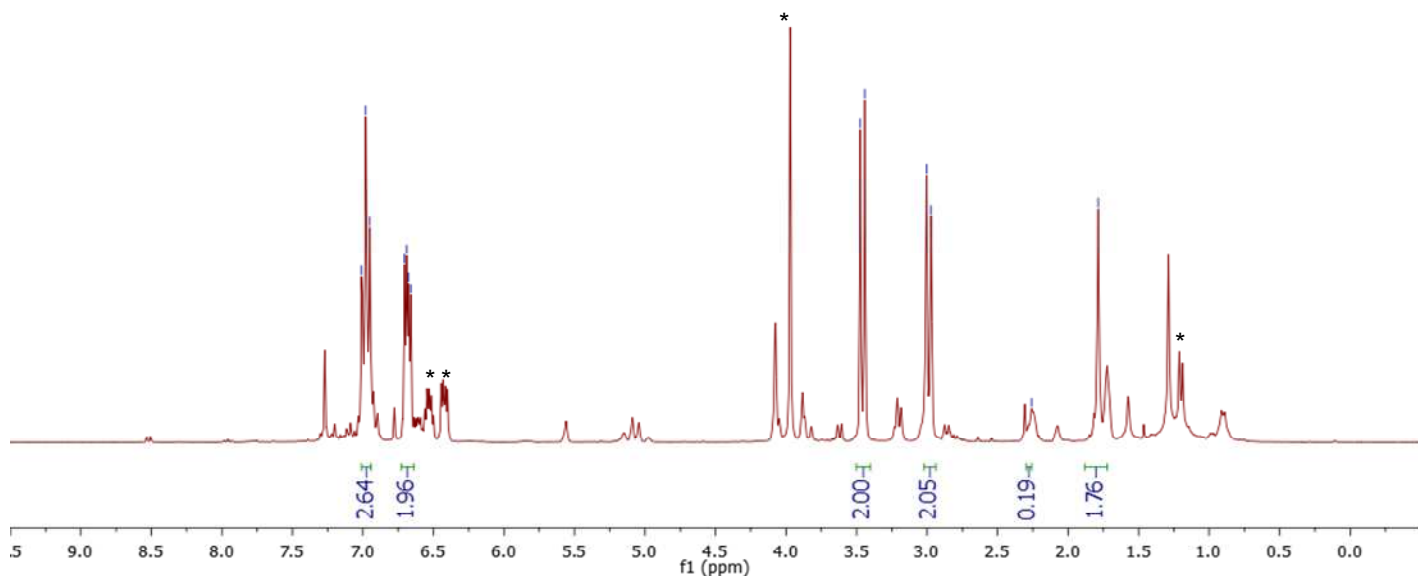
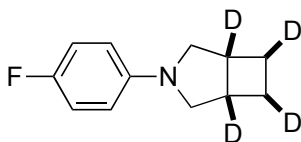




VAS-IV-266refil\_CDCl3\_NB3-10-fid

7.03, 6.88, 6.80, 6.68, 6.66, 3.47, 3.44, 3.00, 2.97, -2.26, -1.79

\*d<sub>8</sub> N,N-dipropyl-4-fluoroaniline



VAS-IV-266refilquant\_A2-106-106fid  
quant13Cp1.PU CDCl3 /op/Topspin3.0 vschmidt

Quantative <sup>13</sup>C NMR : the triplets at 37 and 24 ppm indicate a single deuterium incorporated at those carbon atoms. No other triplets were identified corresponding to the cyclobutane product.

